DOI: 10.1111/mice.13196

RESEARCH ARTICLE

COMPUTER-AIDED CIVIL AND INFRASTRUCTURE ENGINEERING WILEY

Multi-network coordinated charging infrastructure planning for the self-sufficient renewable power highway

Tian-Yu Zhang[1] | **En-Jian Yao**[1] | **Yang Yang**[1] | **Hong-Ming Yang**[2] | **David Z. W. Wang**[3]

[1]Key Laboratory of Transport Industry of Big Data Application Technologies for Comprehensive Transport, Beijing Jiaotong University, Beijing, China

[2]Hunan Provincial Engineering Research Center of Electric Transportation and Smart Distributed Network, Hunan Provincial Key Laboratory of Smart Grids Operation and Control, School of Electrical Engineering and Information, Changsha University of Science and Technology, Changsha, China

[3]School of Civil and Environmental Engineering, Nanyang Technological University, Singapore, Singapore

Correspondence
En-Jian Yao, Key Laboratory of Transport Industry of Big Data Application Technologies for Comprehensive Transport, Beijing Jiaotong University, Beijing, China.
Email: enjyao@bjtu.edu.cn

Funding information
Fundamental Research Funds for the Central Universities, Grant/Award Number: 2023YJS151; National Natural Science Foundation of China, Grant/Award Numbers: 52172312, 71931003; Singapore Ministry of Education Academic Research Fund (AcRF), Grant/Award Number: Tier 1 project RT22/22

Abstract

Developing a self-sufficient renewable power (RP) road transport (SRPRT) system is an important future direction for transport–energy integration. More well-developed studies must be conducted on the coordinated planning of transport, power supply, and power generation networks. This paper carries out the joint operation and planning of highway charging networks with the wind-photovoltaic-energy storage (HCN-WPE) system. Under multi-network integration and the interaction among multiple entities, a nested bi-level optimization model is proposed to optimize the users' charging and travel behavior, charging network's deployment, and power generation system's (PGS) configuration. An H-M-L algorithm structure is developed, combining the heuristic algorithm, multi-agent-based simulation technology, and linear programming algorithm. Its convergence and applicability are verified on the Nguyen-Dupius network. An empirical case in the Hu-Bao-Wu city agglomeration in China is employed to explore and discuss the managerial insights for the HCN-WPE system. The study finds that multi-network coordinated planning can improve the benefits of multiple entities, where the net present value, RP supply rate, and RP consumption rate increase by 12.0%, 3.2%, and 10.5%, compared to independent planning. Network-level planning can play a management and induction role in balancing the station's load pressure. In addition, the PGS co-configuration can leverage the complementary power supply of multiple RP generators and the peak cutting and valley filling of energy storage systems, which is essential for achieving the SRPRT goal.

1 | INTRODUCTION

In the Net Zero Emissions by 2050 Scenario, electrification of transport and cleaner energy are two important directions. By 2030, the shares of renewable energy (RE) are expected to rise from close to 5% to 17%, and more than 50% of the passenger cars sold are electric (IEA, 2023). Therefore, China proposes to build a green, self-sufficient renewable power (RP) and sustainable transportation and energy integration system to achieve low-carbon transportation (CPC Central Committee and the State Council, 2019; National Development and Reform Commission,

2022). In the preliminary transport and energy integration phase, the highway will strive to build a self-sufficient RP road transport (SRPRT) system (China Energy, 2022; Xia et al., 2022). By tapping into the wind–solar RE resources and land resources carried by the highway, the SRPRT system will act as both an energy producer and a service provider for the en-route charging demands of electric vehicle (EV) users. Therefore, to achieve the goal of SRPRT, the highway charging network with the wind-photovoltaic (PV) energy storage (HCN-WPE) system has been brought up, which could effectively exploit the combined advantages of "transportation + energy" (Li et al., 2022). On the transportation side, incorporating low-cost and clean RE could reduce the energy costs of the transport network and reach the full potential of clean energy in the transport infrastructure. On the energy side, the demand managing and inducing role of transport infrastructure could enhance the local consumption level of RP power and promote the efficient utilization of power generation facilities.

Existing explorations regarding the joint operation and planning of the HCN-WPE system in multi-network coordination are still being determined (Unterluggauer et al., 2022). Most results separated the transport network planning from the energy system planning (Gan et al., 2021; Q. Sun et al., 2022). In transportation, the research objects are mostly power supply facilities (i.e., the charging station) only. They focus on the matching problem between the charging demand and facilities service (T. Y. Zhang et al., 2023). The type of energy supply, the richness of natural resources, and the configuration of power generation facilities are ignored. In the energy field, the planning of power generation facilities is mainly conducted for an individual district (Nishanthy et al., 2022; B. Zeng et al., 2020) or small regional networks (Henrique et al., 2023), ignoring the role of the infrastructure network in managing and inducing users' travel and replenishment behavior in space and time. The independence of transportation and energy planning leads to the following two limitations of the obtained deployment scheme. On the one hand, limited by local natural resources, the power mismatch between power supply facilities and generation facilities could occur in the actual operation and planning of the station. On the other hand, it is difficult to exploit the full potential of the highway's RP development. These problems will be more evident driven by the goal of SRPRT.

The HCN-WPE system proposed in this study involves three main entities: EV users, power supply facilities (charging station), and power generation facilities (wind, PV, energy storage system [ESS]). In the stage of operation and planning, they are not independent of each other but interact in a stepped manner. As intermediaries for power transmission, charging stations consider both the replenishment demands of EV users and the power generation capacity of the wind-PV-ESS (WPE) system in their operation and planning. On the one hand, the charging facilities should provide a high level of service (LOS) for the en-route charging demands of EV users (T. Y. Zhang et al., 2022). On the other hand, the deployment of charging networks should accommodate the local RE resources to achieve the SRPRT goal. Conversely, the deployment of charging networks affects EV users' travel and replenishment behavior, which in turn impacts the load demand of power supply and generation facilities (Mowry & Mallapragada, 2021).

To achieve the SRPRT goal, a nested bi-level optimization model is proposed in this study for the joint operation and planning of the HCN-WPE system. At the operational level, the study simulates and models the decision-making process of EV users to determine the en-route charging demand, flow transmission, charging system service operation, and multiple power exchanges. This enables the dynamic interaction of the information flow, energy flow, and traffic flow within the HCN-WPE system. At the planning level, considering the limitations of RE, the LOS of power supply facilities, and the accessibility of the charging network, the deployment of the HCN-WPE system is optimized to obtain the maximum net present value (NPV). The optimized objects include the location and capacity of charging stations and the installed capacity and rated power of the WPE system. For solving the joint operation and planning problem, an algorithm structure based on a heuristic algorithm, multi-agent-based (MA) simulation technology, and linear programming (LP) algorithm, abbreviated as the H-M-L algorithm, is developed. The convergence and applicability of the proposed H-M-L algorithmic structures are verified on the Nguyen-Dupius network. Then, the "Hu-Bao-Wu" urban agglomeration in Inner Mongolia is selected as a real case to explore and discuss the managerial insights for the HCN-WPE system.

The contributions of this study are summarized as follows:

1. A nested bi-level optimization model is established for the coordinated planning of charging network deployment and WPE system configuration. This model considers the interests of EV users, power supply facilities, and power generation facilities. As a result, the HCN-WPE system can achieve optimum economy and energy benefits overall.
2. The proposed optimization model enables the joint operation and planning for the HCN-WPE system. By dynamically interacting and transmitting traffic flow, power flow, and information flow within the HCN-WPE system, the HCN-WPE deployment is optimized based on the daily operation status. This ensures that the

replenishment service in the final HCN-WPE system is sustainable with high LOS in actual operation.
3. An H-M-L algorithm structure is developed to solve the proposed model. It embeds the MA simulation technology and LP algorithm into the heuristic algorithm. It is a helpful algorithm structure for solving large-scale multi-network joint operation and planning problems.

The remainder of this paper is arranged as follows. The related studies are reviewed in Section 2. The problems are described in Section 3. The model formulation and solution technique are illustrated in Sections 4 and 5, respectively. Then, an empirical study is discussed in Section 6. Last, the findings and future research are concluded in Section 7.

2 | LITERATURE REVIEW

2.1 | Deployment optimization of charging network

There are two streams of research on the deployment optimization of charging networks, depending on the method of estimating charging demand (Kchaou-Boujelben, 2021). One stream is the node-based deployment model (T. Zeng et al., 2019; T. Y. Zhang et al., 2023). This category of models usually has evolved from the traditional P-Median, P-Center, MCLP, and so forth. The discrete node-based charging demands are obtained based on global positioning system data, dwell patterns, point-of-interest data, and so forth. The node-based deployment model is suitable for intra-city charging network planning, where the road network is complex and highly precise vehicle data are available. The other stream is the flow-based deployment model (Hajibabai et al., 2023; X. Zhang et al., 2018). The typical model structure of this category is a bi-level optimization model (He et al., 2018), with an upper model for deployment optimization and a lower model for traffic flow assignment. The flow-based charging demands are captured by modeling users' driving process on the road. This category of the model is suitable for highway charging network planning because it has a simple road structure but limited vehicle data, mostly origin and destination (OD) flow data.

However, current explorations regarding the deployment optimization of highway charging networks should be improved in the following aspects: (i) It is necessary to accurately assess the facilities' real-time operational status in the planning stage (Domínguez-Navarro et al., 2019; T. Y. Zhang et al., 2022). Existing research has mostly used the static traffic assignment combined with mathematical queuing theory as the lower model (Gan, Shahidehpour, Guo, et al., 2020; W. Yang et al., 2020). They ignore the dynamic differences in EV users' travel and charging behavior caused by the dynamically changed LOS of the service system. This will cause great difficulties in ensuring the sustainable operation of the charging network services throughout the day in the actual working of the planned scheme (Zhao et al., 2021). (ii) In past studies on charging network deployment, the energy benefits were less considered. The energy benefits are mostly used as indicators for deployment scheme evaluation (T. Y. Zhang et al., 2023) instead of as decision indicators in the planning stage of the charging network. It will lead to an eventual mismatch between the power supply and generation systems, making it difficult to achieve the goal of SRPRT.

2.2 | Configuration optimization of power generation system (PGS)

In recent years, some investigators have been working on the problem of configuration optimization of the PGS to promote power cleanliness on the energy side (B. Sun, 2021). The configuration of the energy system is optimized based on the coordinated operation of power generators and ESS.

However, the research about the coordinated configuration optimization of the PGS is still at an initial stage and has two main limitations to develop. (i) Few studies have considered the interaction between the PGS's planning and users' travel and replenishment behavior. Most researchers have optimized the configuration for individual energy parks with fixed load curves (Nishanthy et al., 2022; B. Zeng et al., 2020). While in reality, users' decision-making behavior for travel and charging is affected by the deployment of the charging network. Further, some researchers have optimized the PGS's configuration on small regional networks (Henrique et al., 2023; Q. Sun et al., 2022). However, they modeled user demand decisions by traditional models such as the gravity model, shortest path model, and static traffic assignment, which make it hard to establish the dynamic interaction between users and users and users and facilities. (ii) The coordinated planning of the PGS is a critical approach to mitigate the intermittency of a single natural resource. Still, only a few studies have been conducted to explore how the multiple involved facilities work dynamically and together (Nguyen et al., 2021; Nishanthy et al., 2022). The advantages of complementary power generation from multiple REs and the role of energy storage devices in peak-shaving and valley-filling have not been fully appreciated.

TABLE 1 Comparison of this study with recent studies on multi-network coordinated planning.

		Transport network		Power supply network		Power generation network		
Refs	Methods	Flow transmission	Users' demand response	Deployment	Charging service	Single RE	Multiple REs	ESS
Gan, Shahidehpour, Yan, et al. (2020)	MINLP	√	×	√	✗	✗	✗	√
Q. Zhang et al. (2023)	MINLP	✗	√	√	√	✗	✗	✗
Gan et al. (2021)	Two-stage stochastic planning	√	✗	√	✗	√	✗	√
Henrique et al. (2023)	Two-stage optimization	✗	✗	√	✗	√	✗	✗
Ali et al. (2022)	Bi-level metaheuristic solution	✗	√	✗	✗	✗	√	✗
T. Y. Zhang et al. (2022)	Bi-level optimization	√	√	√	√	✗	✗	✗
This study	Nested bi-level optimization	√	√	√	√	✗	√	√

Abbreviations: ESS, energy storage system; MINLP, mixed integer nonlinear programming; RE, renewable energy.

2.3 | Coordinated planning of multi-network

In pursuing the maximization of the common interests of multiple entities, many researchers study the coordinated planning of multiple networks for charging network deployment. The joint operation and planning of the charging network involve the dynamic interaction of transportation, power, and energy networks.

At the transport network level, the focus is on the LOS of charging facilities. The evaluation indicators include service coverage, number of served vehicles, users' waiting or detour time, and so forth. At the power network level, the impact of charging loads on the grid, such as power supply reliability and power quality, is focused on. Some researchers have carried out the coordinated deployment optimization of transport and power system networks (Azin et al., 2021; Ferro et al., 2021; Wang et al., 2018). The typical model structure combines a demand estimation model with the power flow model. At the energy network level, some researchers have optimized the PGS's configuration to improve the system's energy benefits (Ali et al., 2022; Li et al., 2022). Due to insufficient attention to the environmental and energy benefits, there are fewer studies on the coordinated planning of transport and energy networks. With the coupling of the transport network, hydrogen network, and power distribution network, Gan et al. (2021) carried out the deployment of a hydrogen network, that is, hydrogen pipelines, hydrogen refueling station, RE generator, and power to the gas device.

Table 1 compares this study with recent studies on multi-network coordinated planning, which provide the foundation and inspiration for this study. Overall, the recent studies suffer from the following shortcomings: (i) There is less coordinated planning for transport, power supply, and power generation networks. They mostly involve the coupling of two networks, failing to take full advantage of the demand-inducing benefits of charging networks and the energy benefits of RE. (ii) In the network planning stage, the real-time demand response of users and operating status changes of facilities are not sufficiently considered. It is difficult to guarantee that charging facilities and power generators can provide a sustainable and satisfactory LOS to EV users. (iii) Most power generation planning is for a single RE or ESS, ignoring the complementary effect of multiple REs and the co-configuration effect of RE generators and ESSs.

3 | PROBLEM DESCRIPTION AND NOTATIONS

In this section, we first propose a hierarchical and coordinated operation mode for the HCN-WPE system. Subsequently, the framework of the nested bi-level optimization model is elaborated.

3.1 | Operation mode

Affected by natural resources, distributed RP generation is highly volatile and intermittent. The instability of RP sources leads to various safety issues such as voltage fluctuations, flicker, and harmonics after grid connection.

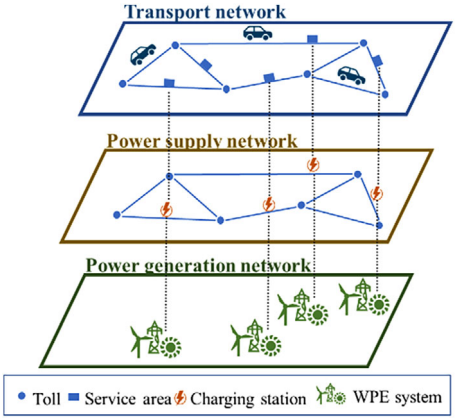

FIGURE 1 The operation mode for the highway charging network with the wind-photovoltaic (PV)-energy storage system (ESS; HCN-WPE) system.

Therefore, a hierarchical and coordinated operation mode for the HCN-WPE system is established to avoid safety issues. Its framework is displayed in Figure 1.

The HCN-WPE system is an energy system with power supply and generation facilities on the highway. The transport network comprises highway tolls, service areas, and roads. The power supply network is made of charging stations built in the service areas and connected along the highway. The charging stations work interconnected to provide sustainable charging services. The real-time road status and charging facilities' working conditions are transmitted simultaneously to the information cloud platform (Liu et al., 2013). Subsequently, the HCN-WPE system provides real-time travel and replenishment solutions for EV commuters. The coordinated operation of the charging stations enables the management of charging demand at the network level and enhances the stability of the power supply network. The individual charging station is equipped with a local PGS integrating wind and PV generators, ESS, variable current equipment, and so forth. Due to the long distances between motorway service areas and to avoid the security effects of distributed power generation on the local grid (Fathabadi, 2020), the distributed PGS operates independently to meet the local load.

Overall, the proposed operation mode for the HCN-WPE system combines the advantages of demand management and induction of the power supply network and the safe and independent operation of the individual PGS. It is noted that this mode is especially suitable for highways that span a large scale, with abundant natural resources but weak power grids.

3.2 | Model framework

This section performs a nested bi-level optimization model for joint operation and planning of the HCN-WPE system based on the above operation mode. The framework is presented in Figure 2.

The planning model is nested by two bi-level optimization models: the dynamic traffic assignment (DTA)-based deployment model for the charging network (orange zone) and the coordinated configuration model for the WPE system (blue zone). The nested part is the shared upper model. The lower model A in the orange zone is the MA-DTA model. Under the charging network deployment, the EV users' travel and energy replenishment behavior and charging stations' operation are modeled and simulated. It captures the discrete and differentiated en-route charging demands of EVs and real-time stations' LOS, which are the foundation of lower model B and upper model. The lower model B is the WPE system configuration model in the blue zone. Based on the load demand under the charging network and the local RE resources, the configuration of wind and PV generators and ESSs are optimized to maximize the NPV of the individual WPE system. Inputting the charging demand and network's LOS from the lower model A and the PGS's configuration from the lower model B, the upper model optimizes the location and capacity of charging stations to maximize the NPV of the HCN-WPE system.

The three main advantages of the proposed nested bi-level optimization model are: (i) Realizing the coordinated multi-network planning of the HCN-WPE system. This optimization model effectively decomposes power supply and generation facilities plannings within the hierarchical and coordinated operation mode. (ii) Realizing the joint operation and planning of the HCN-WPE system. The dynamic interaction of human-vehicle-road-facility-information provides reliable charging demand estimation and network status assessment for the deployment planning of the HCN-WPE system. (iii) The model comprehensively considers the multiple interests of travelers, power supply facilities, and power generation facilities. From travelers' perspective, EV charging demand under the network in the stochastic dynamic user equilibrium (SDUE) status is obtained. In deploying power supply facilities, the charging network's management and induction role on EV users' replenishment demands is played to achieve the maximum NPV of the HCN-WPE system. In the configuration of power generation facilities, wind and PV generators and ESS are planned coordinately with the guidance of SRPRT.

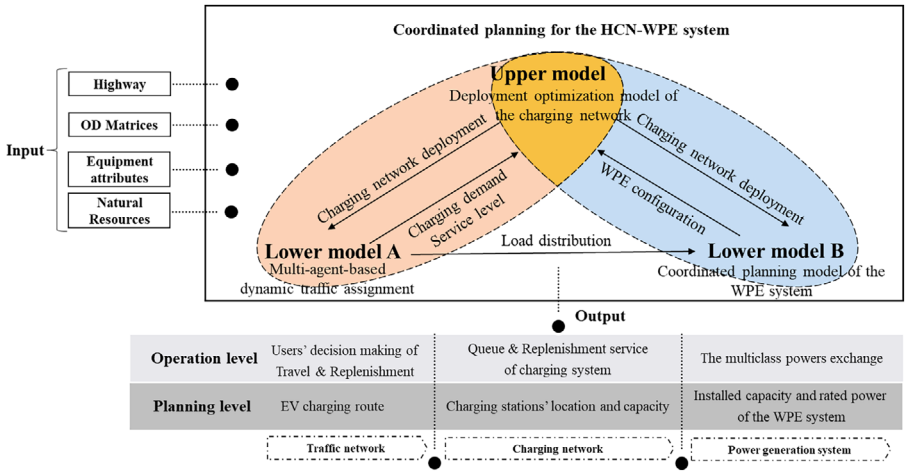

FIGURE 2 The framework of the nested bi-level optimization model. EV, electric vehicle; OD, origin and destination.

3.3 | Notation and assumptions

The network of highways with charging facilities is defined as (N, R). N is the network of highways, which consists of the set of origin and destination O, D, the set of road sections A, and the location of service areas ϕ, where $\phi \in A$. R is the charging network. The $\phi(R)$ is the location of charging stations, where $\phi(R) \in \phi$. The sets of simulation periods in the lower model A and model B are T and T', respectively. X is the set of EVs. And X_t is the set of EVs in the network at time t.

As the agent, each EV $x \in X$ is labeled with its static characteristics and dynamic characteristics. Take EV x as an example, and its static information is represented as $S_x = \{S^0, (o_x, d_x), t_x, L_x = \{o_x, \dots, k_x, k_x + 1, \dots, c_x, \dots, d_x\}\}$, which in order represent the initial status of charge (SOC), origin and destination, departure time, and route, respectively. The travel route L_x is composed of nodes $K_x = \{o_x, \dots k_x, k_x + 1, \dots, d_x\}$ and charging stations $C_x = \{\dots, c_x, \dots\}$ that it passes through in sequence. With the introduction of the time variable t, the dynamic information is represented as $D_{x,t} = \{k_{x,t}, SOC_{x,t}, status_{x,t} = \{C, D\}, f\_time_{x,t}\}$, which includes current location $k_{x,t}$, battery SOC $SOC_{x,t}$, vehicle status $status_{x,t} = \{C, D\}$, and the length of time to end the current status $f\_time_{x,t}$. Vehicle status C and D indicate the charging and driving statuses, respectively. And its corresponding $f\_time_{x,t}$ indicates the remaining time for the vehicle to leave the charging station or the road. Detailed explanations of notation can be found in the Appendix. Before modeling, some assumptions are explained below:

Assumption 1. With the advanced communication technology, EV users can keep informed of the real-time status of the transport and charging networks.

Assumption 2. Ignores the heterogeneity of vehicles and users, that is, all vehicles have the exact attributes, and all users have the same perception of value.

Assumption 3. Due to the long distance between the highway service areas and economic and safety considerations, the power generation facilities at each station are operated independently.

4 | MODEL FORMULATION

4.1 | Lower model A

Taking the highway, charging network, and the real-time OD matrix as input, the lower model A simulates the dynamic processes of EV charging demand response, station queuing service, and traffic flow transmission with EV users' travel path as the decision variable. Finally, the spatial-temporal matrix of charging demand and LOS for charging stations on the network in the SDUE status is obtained.

4.1.1 | EV route searching

First, the EV route set accounting for the en-route charging demands is constructed based on the highway topology network and charging station deployment. Precisely, to reflect the driving range anxiety of EV users during highway driving and the energy demand for the second trip after leaving the highway, parameters S^1 and S^2 are introduced to indicate the minimum SOC thresholds that the EV could accept while driving and leaving the

highway, respectively. As a result, within the network of the highway N and the charging network R, the set of effective routes for EV users between (o, d) is denoted by $L^e_{o,d}(N, R)$, and its functional expression is formulated by Equation (1).

$$L^e_{o,d}(N,R) = f^e\left(S^0, S^{\exp}, S^1, S^2, L^g_{o,d}(N), R, n\right) \quad \forall o \in O, d \in D \tag{1}$$

where the parameters S^0 and $S^{\exp}$ are the initial SOC and the expected SOC after leaving the charging station, respectively; $L^g_{o,d}(N)$ is the set of routes from o to d on highway N for gasoline vehicles, obtained by Dijkstra's algorithm and Depth-First algorithm. In long-distance trips, EV users could charge several times en-route. The parameter n indicates the maximum number of charging times.

4.1.2 | EV users' decision-making

At the departure time, EV users determine their travel and charging route based on the status of the road network and charging network at the current moment and their travel preferences. A path size logit model models the decision-making process as shown in Equations (2)–(4). The probability of route choice for EVs is calculated by Equation (2). Equations (3) and (4) calculate the generalized travel cost $TC_{x,l}(R)$ and correction term $M_{o,d,l}$ of the corresponding route, respectively. The minimum expected travel cost on (o, d) at time t, $\mu^t_{o,d}(R)$ is calculated by Equation (5).

$$PC_{x,l}(R) = \frac{\exp\left[-\theta \cdot TC_{x,l}(R) + \ln(M_{o,d,l})\right]}{\sum_{l \in L^e_{o,d}(N,R)} \exp\left[-\theta \cdot TC_{x,l}(R) + \ln(M_{o,d,l})\right]} \forall x \in X \tag{2}$$

$$TC_{x,l}(R) = \sum_{a \in l} \alpha \cdot \tau_{a,t} + \sum_{c_i \in C_x} \left[\beta \cdot H_{x,c_i}(R) + (TW_{x,c_i}(R) + TC_{x,c_i}(R)) \cdot \alpha\right] \quad \forall x \in X \tag{3}$$

$$M_{o,d,l} = \sum_{a \in l}\left(\frac{\Delta l_a}{\Delta l_l} \cdot \frac{1}{\sum_{l \in L^e_{o,d}(N,R)} \partial_{a,l}}\right) \quad \forall o \in O, d \in D, l \in L^e_{o,d}(N,R) \tag{4}$$

$$\mu^t_{o,d}(R) = -\frac{1}{\theta}\ln\left[\sum_{l \in L^e_{o,d}} \exp\left(-\theta \cdot TC_{x,l}(R)\right)\right] \quad \forall r \in O, s \in D, t \in T \tag{5}$$

where $TC_{x,l}(R)$ is the generalized travel cost of route l for EV x under the charging network R; $\tau_{a,t}$ is the travel time of road a at time t. $H_{x,c_i}(R)$, $TW_{x,c_i}(R)$, and $TC_{x,c_i}(R)$ are the charging volume, queuing time, and charging time of EV x at charging station c_i, respectively; α and β are the time value of EV users and charging price; $PC_{x,l}(R)$ is the probability that EV x chooses route l. θ is a discrete coefficient reflecting user perception differences; $M_{o,d,l}$ is the correction term of route l; Δl_a and Δl_l are the lengths of road a and route l; $\partial_{a,l}$ is the binary variable to judge whether road a is part of route l. If it is, then $\partial_{a,l} = 1$; otherwise, $\partial_{a,l} = 0$.

4.1.3 | Charging system service modeling

Each charging station is also labeled. Its static characteristic is the number of chargers B_i. Its dynamic characteristic indicates the station's real-time operation status, that is, the remaining working time of each charger at the current moment. $t^{\text{pile}}_{c_i,b,t}(R)$ indicates the working finishing time of charger b at charging station c_i at time t. When the EV arrives at the charging station, its status $status_{x,t}$ alters from D to C. Based on the current operating status, the EV user selects the charger with the shortest remaining working time to queue and charges until the battery SOC up to $S^{\exp}$, then leaves the station. The mathematical modeling of this queuing service system is presented in Equations (6)–(8). The departure moment $t^{\text{l}}_{x,c_i}(R)$, queuing time $TW_{x,c_i}(R)$, and charging time $TC_{x,c_i}(R)$ at the charging station are calculated by Equations (6), (7), and (8), respectively.

$$t^{\text{l}}_{x,c_i}(R) = t^{\text{a}}_{x,c_i}(R) + TW_{x,c_i}(R) + TC_{x,c_i}(R) \quad \forall x \in X, c_i \in C_x \tag{6}$$

$$TW_{x,c_i}(R) = \max\left\{0, \min_{b \in B_i}\left\{t^{\text{pile}}_{c_i,b,t}(R)\right\} - t^{\text{a}}_{x,c_i}(R)\right\} \quad \forall x \in X, c_i \in C_x \tag{7}$$

$$TC_{x,c_i}(R) = 50\ln\left[\left(S^{\exp} - S_{x,c_i}(R)\right)/0.9371 + 1\right] \quad \forall x \in X, c_i \in C_x \tag{8}$$

where $S_{x,c_i}(R)$ denotes the SOC of EV x arriving at the charging station c_i; $t^{\text{a}}_{x,c_i}(R)$ and $t^{\text{l}}_{x,c_i}(R)$ are the moments when x arrives and leaves the station c_i, respectively.

4.1.4 | Dynamic traffic flow transmission

In this section, the link transmission model models the dynamic driving process of EVs on the highway. The transport network reaches the SDUE status when the travel costs of the selected routes in any OD pair are equal and not greater than that of the other routes. The formulation of the SDUE status is as follows.

$$\sum_{o\in O}\sum_{d\in D}\sum_{t\in T}\sum_{l\in L^e_{o,d}(N,R)} v^t_{o,d,l}\cdot\left[TC_{x,l}(R)-\mu^t_{o,d}(R)\right]=0 \quad (9)$$

$$\begin{cases} TC_{x,l}(R)-\mu^t_{o,d}(R)\geq 0 \\ v^t_{o,d,l}\geq 0 \end{cases} \quad (10)$$

where $v^t_{o,d,l}$ is the inflow rate of choosing route l on (o,d) at time t.

The DTA model follows the constraints below: During the flow transmission, the transport network must ensure that the inflow/outflow is conserved and satisfies the road capacity. Equation (11) updates the number of vehicles on the road dynamically. It is important to note that as the charging events occur in the service area, this part of the EV does not affect the traffic status of the road. Equations (12) and (13) calculate each road's real-time outflow and inflow rates. To describe the flow dynamic transmission characteristics of the link, a discrete flow transmission constraint is established as shown in Equation (14). Equation (15) indicates that the road outflow rate relies on the road inflow rate and the restricted capacity. Equation (16) is the flow conservation constraint for the node. Furthermore, other general constraints are expressed by Equation (17).

$$X^t_a=\begin{cases} X^{t-1}_a+\left(u^t_a-v^t_a\right)T/S' & a\notin\phi \\ X^{t-1}_a+\left(u^t_a-v^t_a\right)T/S'+d^{t-1}_a-d^t_a, & a\in\phi \end{cases}$$
$$\forall a\in A, t\in T \quad (11)$$

$$u^t_a=\sum_{o,d}\sum_{l\in L^e_{o,d}(N,R)} u^t_{o,d,l}\cdot\partial_{a,l} \quad \forall a\in A, t\in T \quad (12)$$

$$v^t_a=\sum_{o,d}\sum_{l\in L^e_{o,d}(N,R)} v^t_{o,d,l}\cdot\partial_{a,l} \quad \forall a\in A, t\in T \quad (13)$$

$$v^{t+\tau^t_a}_a=\frac{u^t_a}{1+\left(\tau^t_a-\tau^{t-1}_a\right)/\Delta t} \quad \forall a\in A, t\in T \quad (14)$$

$$v^{t+\tau^t_a}_a=\begin{cases} C_a & \tau^t_a>t_a \\ u^t_a, & \tau^t_a\leq t_a \end{cases} \quad \forall a\in A, t\in T \quad (15)$$

$$\sum_{a\in EE(o)} v^t_a=\sum_{d\in D}\sum_{l\in L^e_{o,d}(N,R)} f^t_{o,d,l}+\sum_{a\in ES(o)} u^t_a \quad \forall o\in O \quad (16)$$

$$u^t_a\geq 0, v^t_a\geq 0, \tau^t_a\geq 0 \quad \forall a\in A, t\in T \quad (17)$$

where $u^t_{o,d,l}$ is the outflow rate of choosing route l on (o,d) at time t. X^t_a is the number of vehicles on road a at time t; u^t_a and v^t_a are the outflow rate and inflow rate of road a at time t; d^t_a is the number of EVs at charging station built on road a at time t; C_a and t_a are the capacity and the free-flow travel time of road a; $EE(o)$ and $ES(o)$ are the set of road ending and starting at node o, respectively; $f^t_{o,d,l}$ is the new loading flow choosing route l on (o,d) at time t; Δt is the time step.

To prove the existence of a feasible solution, the variational inequality (VI) of the SDUE problem is formulated as Equation (18). Where $q^t_{o,d}$ is the new loading flow on (o,d) at time t, the variable $f^{t,*}_{o,d,l}$ with superscript * is the optimal solution. The feasible domain of the model is $\Omega=\{\text{Equations (6)}\sim(8),(11)\sim(17)\}$. According to the complementary relaxation Karush–Kuhn–Tucker condition, Equation (19) can be derived when $f^{t,*}_{o,d,l}\geq 0$.

$$\sum_{o\in O}\sum_{d\in D}\sum_{l\in L^e_{o,d}}\sum_{t\in T}\left\{\begin{array}{l} TC_{x,l}(R)\cdot f^t_{o,d,l}+ \\ \frac{1}{\theta}\left[\ln\left(f^{t,*}_{o,d,l}\right)-\ln\left(q^t_{o,d}\right)\right]-\mu^t_{o,d}(R)\end{array}\right\}$$
$$\times\left(f^t_{o,d,l}-f^{t,*}_{o,d,l}\right)\geq 0 \quad (18)$$

$$TC_{x,l}\left(f^t_{o,d,l}\right)(R)+\frac{1}{\theta}\left[\ln\left(f^{t,*}_{o,d,l}\right)-\ln(q^t_{o,d})\right]-\mu^t_{o,d}(R)=0$$
$$\Rightarrow f^{t,*}_{o,d,l}=q^t_{o,d}\cdot\exp(-\theta\cdot TC_{x,l}\left(f^t_{o,d,l}\right)(R)+\theta\cdot\mu^t_{o,d}(R)] \quad (19)$$

Taking $\mu^t_{o,d}$ in Equation (5) into Equation (19), which is consistent with Equation (2), it has been proved that in the equilibrium allocation problem, the VI and its immovable point problem have equivalence (Smith, 1979); the equivalence still holds under dynamic conditions when modeled in a tightly convex set of inflow rates. The model can also be considered an immovable point problem. The variables in this problem are continuous functions, which means that there is a feasible solution available.

4.2 | Lower model B

For the individual WPE, the lower model B optimizes the installed capacity of wind and PV generators and ESS's capacity and rated power coordinately with the mathematical modeling of the dynamic operation of the WPE system.

4.2.1 | Power modeling

In the WPE system, power is supplied to the charging station from four sources: wind generators, PV generators,

ESSs, and the local grid. Next, the mathematical models of the power sources are explicitly described.

The output power of wind generators is related to the local real-time wind speed and installed capacity. Considering the relationship between the operation of the fan and the wind speed, the actual power output $p_{i,t}^{\mathrm{W}}$ of the wind generators at station i in time t could be formulated as in Equation (20):

$$p_{i,t}^{\mathrm{W}} = \begin{cases} 0 & v'_{i,t} < v_{\mathrm{in}} \text{ or } v'_{i,t} \geq v_{\mathrm{out}} \\ IC_i^{\mathrm{W}} \dfrac{v'_{i,t} - v_{\mathrm{in}}}{v_{\mathrm{rate}} - v_{\mathrm{in}}} & v_{\mathrm{in}} < v'_{i,t} \leq v_{\mathrm{rate}} \\ IC_i^{\mathrm{W}} & v_{\mathrm{rate}} \leq v'_{i,t} < v_{\mathrm{out}} \end{cases} \quad \forall i \in \phi(R), t \in T' \tag{20}$$

where IC_i^{W} is the installed capacity of the wind generators at station i, kW; v_{in}, v_{out}, and v_{rate} are the cut-in wind speed, cut-out wind speed, and rated wind speed, respectively, and their size relationship is $v_{\mathrm{in}} < v_{\mathrm{rate}} < v_{\mathrm{out}}$. $v'_{i,t}$ is the wind speed at station i in time t. The real-time wind speed curve is obtained via the free, web-based application of Global Wind Atlas, which provides planners with information on wind energy worldwide.

The output power of PV generators is related to the local solar irradiation, temperature, and installed capacity. The actual power output $p_{i,t}^{\mathrm{PV}}$ of PV generators at station i in time t could be formulated as in Equation (21):

$$p_{i,t}^{\mathrm{PV}} = IC_i^{\mathrm{PV}} \frac{G_{i,t}}{G_{\mathrm{stc}}} \left[1 + k' \left(T_{i,t} - T_{\mathrm{stc}}\right)\right] \forall i \in \phi(R), t \in T' \tag{21}$$

where IC_i^{PV} is the installed capacity of PV generators at station i, kW; $G_{i,t}$ and $T_{i,t}$ are the real-time solar irradiation and temperature at station i in time t; G_{stc} and T_{stc} are the solar irradiation and temperature under the standard conditions; k' is the temperature coefficient, which represents the effect of a unit increase in temperature on the output power of a PV module. The real-time information on solar irradiation is provided by the Solargis company. It is a database on solar resources, including real-time solar irradiation, temperature, meteorology, and geography.

The ESS operates in the constant power mode. The SOC of ESSs in time t could be calculated from the input/output power during the period as formulated in Equation (22):

$$SOC_{i,t+1} = SOC_{i,t} + \frac{\eta p_{i,t}^{\mathrm{E}}}{IC_i^E} \Delta t \quad \forall i \in \phi(R), t \in T' \tag{22}$$

where IC_i^E is the installed capacity of ESSs at station i; $SOC_{i,t}$ is the real-time SOC of ESSs at station i in time t; $p_{i,t}^{\mathrm{E}}$ is the real-time input/output power of ESSs at station i in time t; η is the power efficiency.

4.2.2 | Coordinated operation of WPE system

In the operation of the WPE system, four types of power exchange are involved, which are explained as follows. $p_{i,t}^{\mathrm{R2C}}$ and $p_{i,t}^{\mathrm{R2E}}$ are the input powers from the RP generators to chargers and to the ESS at station i in time t; $p_{i,t}^{\mathrm{E2C}}$ and $p_{i,t}^{\mathrm{G2C}}$ are the input powers from the ESS and the grid to chargers at station i in time t. And $p_{i,t}^{\mathrm{D}}$ is the load demand at station i in time t, which is simulated and counted by the lower model A. IP_i^{E} is the rated output power of ESSs at station i.

For highway service areas with weak power grids and abundant natural resources, the WPE system adopts an SRPRT-oriented coordinated operation strategy. Equations (23)–(28) mathematically express the dynamic operation strategy.

$$p_{i,t}^{\mathrm{D}} = p_{i,t}^{\mathrm{R2C}} + p_{i,t}^{\mathrm{E2C}} + p_{i,t}^{\mathrm{G2C}} \quad \forall i \in \phi(R), t \in T' \tag{23}$$

$$p_{i,t}^{\mathrm{E}} = p_{i,t}^{\mathrm{R2E}} - p_{i,t}^{\mathrm{E2C}} \quad \forall i \in \phi(R), t \in T' \tag{24}$$

$$p_{i,t}^{\mathrm{R2C}} = \min\left\{p_{i,t}^{\mathrm{D}}, p_{i,t}^{\mathrm{W}} + p_{i,t}^{\mathrm{PV}}\right\} \quad \forall i \in \phi(R), t \in T' \tag{25}$$

$$p_{i,t}^{\mathrm{G2C}} = \max\left\{0, p_{i,t}^{\mathrm{D}} - \left(p_{i,t}^{\mathrm{W}} + p_{i,t}^{\mathrm{PV}} + p_{i,t}^{\mathrm{E2C}}\right)\right\} \quad \forall i \in \phi(R), t \in T' \tag{26}$$

$$p_{i,t}^{\mathrm{R2E}} = \min\left\{p_{i,t}^{\mathrm{W}} + p_{i,t}^{\mathrm{PV}} - p_{i,t}^{\mathrm{R2C}}, \max\left\{0, \min\left\{IC_i^E \cdot SOC_{\max} - IC_i^E \cdot SOC_{i,t}, IP_i^{\mathrm{E}}\right\}\right\}\right\} \quad \forall i \in \phi(R), t \in T' \tag{27}$$

$$p_{i,t}^{\mathrm{E2C}} = \min\left\{\max\left\{0, p_{i,t}^{D} - (p_{i,t}^{\mathrm{W}} + p_{i,t}^{\mathrm{PV}})\right\}, \min\left\{IC_i^E \cdot SOC_{i,t} - IC_i^E \cdot SOC_{\min}, IP_i^{\mathrm{E}}\right\}\right\} \quad \forall i \in \phi(R), t \in T' \tag{28}$$

Equations (23) and (24) are the power conservation constraint of chargers and the power conservation constraint of ESS, respectively. Equations (25)–(28) are the mathematical expressions of the transmission relations of the four powers. Based on the principle of prioritizing the RP consumption and reducing the dependence on the grid power, the priority of power supply in the WPE system is RP > ESS power > grid power. Meanwhile, to avoid the safety effects of distributed power generation on the local grid, the power from wind and PV generators is consumed only by the local chargers and ESS.

4.2.3 | The configuration optimization of the WPE system

Considering the goal of sustainable operation and SRPRT, a coordinated configuration optimization model of the WPE system is established to maximize the system's annual NPV. The mathematical formulation is in the following.

$$\begin{aligned}&\max NPV_i^{\mathrm{WPE}}(R)\\&=\sum_{t\in T}365\cdot\left[\left(R^{\mathrm{S}}+R^{\mathrm{EN}}\right)\cdot\left(p_{i,t}^{\mathrm{R2C}}+p_{i,t}^{\mathrm{E2C}}\right)+R^{G}\cdot p_{i,t}^{\mathrm{G2C}}\right]\\&-\sum_{m\in\{\mathrm{W,PV,E}\}}C_{im}\forall i\in\phi(R)\end{aligned}\tag{29}$$

$$C_{i,m}=\begin{cases}\dfrac{IC_i^m\cdot\left(U_m^{\mathrm{A}}+U_m^{\mathrm{C}}-D_m\right)\cdot r\cdot(1+r)^{L_m}}{(1+r)^{L_m}-1}\\\quad+IC_i^m\cdot\left(M_m^{\mathrm{A}}+M_m^{\mathrm{C}}\right)\quad\forall m\in\{\mathrm{W,PV}\},i\in\phi(R)\\\dfrac{\left(IP_i^m\cdot U_m^{\mathrm{A}}+IC_i\cdot U_m^{Q}+IP_i^m\cdot U_m^{\mathrm{C}}\right)\cdot r\cdot(1+r)^{L_m}}{(1+r)^{L_m}-1}\\\quad+IP_i^m\cdot\left(M_m^{\mathrm{A}}+M_m^{\mathrm{C}}\right)\quad\forall m\in\{\mathrm{E}\},i\in\phi(R)\end{cases}\tag{30}$$

$$\sum_{t\in T'}\frac{p_{i,t}^{\mathrm{R2C}}+p_{i,t}^{\mathrm{E2C}}}{p_{i,t}^{\mathrm{D}}}\geq\mu'\quad\forall i\in\phi(R)\tag{31}$$

$$SOC_{i,t=0}=\delta'\cdot IC_i^{E}\quad\forall i\in\phi(R)\tag{32}$$

$$SOC_{i,t=23}\geq SOC_{i,t=0}\quad\forall i\in\phi(R)\tag{33}$$

$$\begin{aligned}&IC_i^{\mathrm{W}}\leq IC_{\max}^{\mathrm{W}},IC_i^{\mathrm{PV}}\leq IC_{\max}^{\mathrm{PV}},IC_i^{\mathrm{E}}\leq IC_{\max}^{\mathrm{E}},\\&0.2IC_i^{\mathrm{E}}\leq IP_i^{E}\leq 0.5\quad IC_i^{\mathrm{E}}\forall i\in\phi(R)\end{aligned}\tag{34}$$

where $NPV_i^{\mathrm{WPE}}(R)$ is the NPV of the WPE system at location i; $C_{i,m}$ represents the annual investment and operation and maintenance (O&M) cost of device m; The W, PV, and E in the set {W, PV, E} represent wind generators, PV generators, and ESS respectively; U_{W}^{A} and U_{PV}^{A} in order denote the costs per unit of installed capacity for wind and PV generators, respectively; U_E^A and U_E^Q are the costs per unit of rated power and of installed capacity of the ESS, respectively; U_m^C and D_m in order represent the investment cost of the converter and the equipment salvage value for each device; M_m^{A} and M_m^{C} are the annual O&M costs of the units and converters of device m, respectively; R^{S} and R^G denote the net benefits per unit of sold electricity from RP generators and the grid, respectively; R^{EN} is the environmental benefit per unit of RP. L_m is the lifespan of each device; r is the funding discount rate. To avoid the battery degradation caused by overcharging and over-discharging, $SOC_{\min}$ and $SOC_{\max}$ are set as the lower and upper thresholds of SOC for the ESS in operation, respectively. μ' is the RP supply rate set by the government; δ' is the initial SOC of ESSs during the day.

As illustrated in Equation (29), the annual NPV of the WPE system includes the costs and benefits in both planning and operation. At the planning level, each device's annual construction investment costs and annual operation/maintenance costs are calculated by Equation (30). Take the PV as an example, its average annual investment cost consists of PV generators cost $IC_i^{\mathrm{PV}}\cdot U_{\mathrm{PV}}^{\mathrm{A}}$, converter cost $IC_i^{\mathrm{PV}}\cdot U_{\mathrm{PV}}^{C}$ and salvage value $IC_i^{\mathrm{PV}}\cdot D_{\mathrm{PV}}$; in addition, its annual O&M costs are $IC_i^{\mathrm{PV}}\cdot M_{\mathrm{PV}}^{\mathrm{A}}$ and $IC_i^{\mathrm{PV}}\cdot M_{\mathrm{PV}}^{\mathrm{C}}$. At the operation level, the economic benefits come from electricity sales and environmental benefits, and the costs are for the O&M of each device. For the power cannot be met by RPs, WPS system operators must purchase it from the grid. Therefore, the power sale benefits could be specifically divided into the annual benefits from the electricity sales of RP $\sum_{t\in T}365\cdot[R^{\mathrm{S}}\cdot(p_{i,t}^{\mathrm{R2C}}+p_{i,t}^{\mathrm{E2C}})]$ and that of the grid $\sum_{t\in T}365\cdot R^{G}\cdot p_{i,t}^{\mathrm{G2C}}$. Compared to conventional thermal power plants, RP generators reduce greenhouse gas and pollutant emissions in the power production. The annual environmental benefit is calculated as $\sum_{t\in T}365\cdot[R^{\mathrm{EN}}\cdot(p_{i,t}^{\mathrm{R2C}}+p_{i,t}^{\mathrm{E2C}})]$.

The constraints include power conservation constraints in Equations (23) and (24), operation strategy constraints in Equations (25)–(28), SRPRT constraints in Equation (31), and sustainable operation constraints in Equations (32) and (33). As formulated by Equation (31), the percentage of RP supply within this distributed power supply system is required to be bigger than the preset value μ'. Equations (32) and (33) are set to guarantee the sustainable operation of ESSs, that is, the SOC at the last hour during the day is not less than the initial SOC. Equation (34) is the range constraints for each device's installed capacity and rated power.

4.3 | Upper model

From the investors' view, the upper model optimizes the deployment of charging networks at highways to achieve maximum system economy while guaranteeing comfortable EV travel and realizing the SRPRT goal.

4.3.1 | Charger capacity setting

Wind and solar sources vary greatly in various geographical locations, and this phenomenon is more evident on highways with extensive latitude and longitude spans. Therefore, to ensure that the highway could ultimately

achieve the SRPRT goal, the planner must pre-set the maximum threshold of the charger capacity in the service area before the charging network planning. The calculation formula is in the following.

$$B_{\max,i} = \left\lfloor \frac{T \cdot \sum_{t\in T}\left[p_{i,t}^{\mathrm{W}}\left(IC_{\max}^{\mathrm{W}}\right) + p_{i,t}^{\mathrm{PV}}\left(IC_{\max}^{\mathrm{PV}}\right)\right]}{\Delta t \cdot RP_{\mathrm{ch}} \cdot \mu'} \right\rfloor \forall i \in \phi \tag{35}$$

where $B_{\max,i}$ is the maximum threshold for the number of chargers at the station i; RP_{ch} is the rated power of fast chargers. It is assumed that the station is equipped with the maximum installed capacities of wind generators $IC_{\max}^{\mathrm{W}}$ and PV generators $IC_{\max}^{\mathrm{PV}}$ that the service area could carry. The average maximum hourly power generation at station i is determined by accounting for the local wind and solar conditions and the specified RP supply rate. The integer term of the ratio of this value $T \cdot \sum_{t\in T}[p_{i,t}^{\mathrm{W}}(IC_{\max}^{\mathrm{W}}) + p_{i,t}^{\mathrm{PV}}(IC_{\max}^{\mathrm{PV}})]/(\Delta t \cdot \mu')$ to the rated power of the fast charger is then taken as the maximum threshold for the number of chargers at the station.

4.3.2 | Charging network deployment optimization

The objective function of the charging network optimization model is to maximize the NPV of the HCN-WPE system, that is, the difference between the WPE system's NPV and the charging facility's annual cost as shown in Equation (36). As formulated by Equation (37), the charging facility's annual cost $AC_i^{\mathrm{c}}(R)$ is composed of its average annual construction cost $z_i^{\mathrm{b}}(R)$ and O&M costs $z_i^{\mathrm{oper}}(R)$. Where, as shown in Equation (38), the $z_i^{\mathrm{b}}(R)$ consists of the fixed cost $z_i^{\mathrm{fix}}(R)$ and the variable cost $z_i^{var}(R)$. The $z_i^{\mathrm{fix}}(R)$ is related to whether to build a station or not. And the $z_i^{var}(R)$ is determined by the number of chargers $B_i(R)$ and the capacity of power distribution equipment $S_i^{\mathrm{ET}}(R)$, which is calculated by Equation (39). $z_i^{\mathrm{oper}}(R)$ is composed of the labor cost and the annual O&M cost of the power distribution equipment, which is calculated by Equation (40).

$$\mathrm{Max}\ \ NPV^{\mathrm{HCN-WPE}}(R) = \sum_{i\in\phi(R)}\left[NPV_i^{\mathrm{WPE}}(R) - AC_i^{\mathrm{c}}(R)\right] \tag{36}$$

$$AC_i^{\mathrm{c}}(R) = \frac{z_i^{\mathrm{b}}(R)\cdot r\cdot(1+r)^{L_c}}{(1+r)^{L_c}-1} + z_i^{\mathrm{oper}}(R) \quad \forall i \in \phi(R) \tag{37}$$

$$z_i^{\mathrm{b}}(R) = z_i^{\mathrm{fix}}(R) + z_i^{var}(R) = y_i(R)\cdot z_{\mathrm{cs}} + B_i(R)\cdot z_{\mathrm{ch}} + S_i^{\mathrm{ET}}(R)\cdot z_{\mathrm{tr}} \quad \forall i \in \phi(R) \tag{38}$$

$$S_i^{\mathrm{ET}}(R) = \frac{B_i(R)\cdot K_{\mathrm{ch}}\cdot P_{\mathrm{ch}}}{L_{\max}\cdot\alpha_{\mathrm{cs}}\cdot\eta_{\mathrm{ch}}\cdot\cos\phi_{\mathrm{ch}}} \quad \forall i \in \phi(R) \tag{39}$$

$$z_i^{\mathrm{oper}}(R) = B_i(R)\cdot z_{\mathrm{hr}} + S_i^{\mathrm{ET}}(R)\cdot z_m \quad \forall i \in \phi(R) \tag{40}$$

where $y_i(R)$ is the binary variable to determine whether a charging station is built at station i in the scheme R. If it is built then $y_i(R) = 1$; otherwise, $y_i(R) = 0$. $B_i(R)$ is the number of chargers at station i in the scheme R; $S_i^{\mathrm{ET}}(R)$ is the capacity of power distribution equipment at station i in the scheme R; z_{cs}, z_{ch}, and z_{tr} are the construction cost of the charging station, the construction cost of the charger, and the capacity cost of distribution equipment, respectively; K_{ch} is the simultaneous rate of charging; $L_{\max}$ is the daily maximum load rate of the charging station; α_{cs} is the ratio of charging load to total load at the charging station; η_{ch} is the charging efficiency; $\cos\phi_{\mathrm{ch}}$ is the power factor of chargers; z_{hr} is the average annual labor cost per charger; z_m is the average annual O&M cost per unit of distribution equipment capacity.

Constraints:

1. Facility construction constraints

$$y_i(R) \in \{0,1\} \quad \forall i \in \phi \tag{41}$$

$$y_i(R)\cdot B_{\min} \le B_i(R) \le y_i(R)\cdot B_{\max,i} \quad \forall i \in \phi \tag{42}$$

Equation (41) indicates that charging stations could only be built in alternative service areas. To ensure the system's economy and SRPRT benefits, Equation (42) sets the minimum and maximum thresholds for chargers' capacity.

2. Network accessibility constraint

$$f^e[S^0, S^{\exp}, S^1, S^2, I_{o,d}^g(N), R] \notin \emptyset \quad \forall o \in O, d \in D \tag{43}$$

Equation (43) requires the charging network to support EV users completing trips for any OD pair.

3. System LOS constraints

$$T_i^{\mathrm{avg}}(R) \le T^{\mathrm{avg}} \quad \forall i \in I(R) \tag{44}$$

$$T_i^{\max}(R) \le T^{\max} \quad \forall i \in I(R) \tag{45}$$

The optimization model considers EV users' travel satisfaction and charging facilities' LOS under the charging network. Equation (44) is the normal time LOS constraint, which requires that the average waiting

time for charging vehicles at any station $T_i^{\text{avg}}(R)$ be no higher than T^{avg}. And Equation (45) constrains the peak time LOS of the station by requiring that the maximum waiting time for charging vehicles at any station $T_i^{\max}(R)$ must not be higher than $T^{\max}$.

4. Model relationship constraints

$$(\mathbf{v}(R), \mathbf{f}(R)) = \arg\min_{\mathbf{v},\mathbf{f}} \sum_{t\in T}\sum_{o\in O}\sum_{d\in D}\sum_{l\in K_{rs}^e(R)} TC_x(R) \cdot q_{o,d}^t \cdot P_x(R) \tag{46}$$

$$\left(IC_i^{\text{W}}(R), IC_i^{\text{PV}}(R), IC_i^{\text{E}}(R), IP_i^E(R)\right) = \arg\max_{IC_i^{\text{W}}, IC_i^{\text{PV}}, IC_i^{\text{E}}, IR_i^E} NPV_i^{\text{WPE}}(R) \tag{47}$$

As formulated by Equations (46) and (47), the charging demand and system LOS output from lower model A and the optimal configuration of generation facilities output from lower model B are the inputs to the upper-level model. $\mathbf{v}(R)$ and $\mathbf{f}(R)$ are the matrices of travel and charging decisions when the system reaches the SDUE status in scheme R, respectively. $IC_i^{\text{W}}(R)$, $IC_i^{\text{PV}}(R)$, $IC_i^{\text{E}}(R)$, and $IP_i^E(R)$ are the optimal configurations of WPE system in scheme R.

5 | SOLUTION TECHNIQUE

5.1 | Main algorithm

The inherent complexity of this problem comes from two aspects. First, integrating dynamic operation and planning is challenging. The deployment of the HCN-WPE system is optimized based on the dynamic operation under the multi-networks coordination. Second, the model captures the differentiated charging demands of EV users in great quantity. The lower model A captures EV users' differentiated charging demand information, that is, time, location, and volume, by implementing dynamic simulation on an individual vehicle basis. The simulation efficiency is challenged by the vast number of vehicles on the highway.

Extensive research has demonstrated that heuristic algorithms efficiently and accurately solve various nondeterministic polynomial-hard problems (Hossain et al., 2019; Siddique & Adeli, 2016; Q. Zhang et al., 2023). Therefore, we take the heuristic algorithm as the basic algorithm. In addition, with the high computing speed of the computer, the MA simulation technology could realize the system simulation for large-scale networks with high accuracy. The nonlinear problem is transformed into a linear one, and the LP algorithm obtains its exact solution.

The H-M-L algorithm structure is developed by combining the advantages of the above algorithms and techniques. Next, we construct the genetic algorithm with MA simulation and LP algorithm (G-M-L) algorithm to demonstrate the proposed H-M-L algorithm structure using the genetic algorithm (GA) as a basis, a well-established and widely used heuristic algorithm. Its flow chart is illustrated in Figure 3.

First, pre-processing is executed to calculate the maximum capacity of chargers for each service area by Equation (36). The main procedure of the G-M-L algorithm is as follows. In Step 1, the initial population is encoded by the real-coded method. The lower models A and B are solved sequentially under the current charging network. The MA method of successive averages (MA-method of successive averages (MSA)) algorithm dynamically simulates EV users' travel and replenishment behavior and the queuing service of charging stations under the charging network. Based on the time-of-day load curve of each station, the lower model B is solved by the mixed integer nonlinear programming (MINLP) algorithm. The optimal WPE system configuration under the current charging network is obtained. Next, in Step 2, the finesses of the various deployment schemes are calculated. Then, in Step 3, the new deployment schemes are generated with the facility construction and network accessibility constraints. When reaching the maximum iteration number or when the fitness does not change in the consecutive k iterations, the final deployment solution is obtained.

5.2 | MA-MSA algorithm

An MA-MSA algorithm is developed for solving the DTA model for EV highway trips. The MSA algorithm is used to solve the DTA model in large-scale networks (T. Y. Zhang et al., 2022). Its basic idea is to continuously adjust the network's flow assignment until the network gradually approaches the SDUE status. However, the traditional MSA algorithm cannot capture EV users' en-route replenishment process, a significant component during EVs' highway trips.

Therefore, we embed the MA simulation module into the traditional MSA algorithm. In the simulation module, agents execute their travel route choices and charging decisions sequentially based on the departure time. Through the interaction between vehicles in the road network, the individual travel decisions of EV users are adjusted and executed again, and the optimized travel plan is obtained by iteration. The procedure of the MA-MSA algorithm could be briefly displayed in ALGORITHM 1.

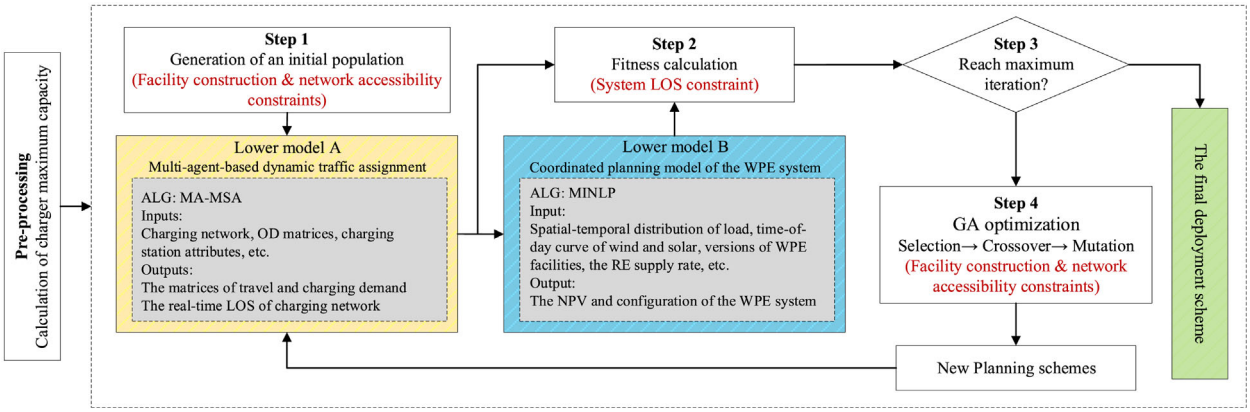

FIGURE 3 The flowchart of the proposed G-M-L algorithm. GA, genetic algorithm; LOS, level of service; MINLP, mixed integer nonlinear programming; OD, origin and destination.

5.3 | Model linearization

Due to the existence of Equations (25)–(29), the lower model B is an MINLP. As a result, this MINLP model is transformed into a mixed integer LP (MILP) model by introducing auxiliary variables combined with the big-M relaxation method. It will enhance the applicability of the model and the accuracy of the corresponding planning results.

The linearization process is explained as an example of Equation (27). By introducing the auxiliary variable $p^1_{i,t}$ and $p^2_{i,t}$, the equation is equivalent to that below.

$$p^{\mathrm{R2E}}_{i,t} = \min\left\{p^{\mathrm{W}}_{i,t} + p^{\mathrm{PV}}_{i,t} - p^{\mathrm{R2C}}_{i,t}, p^1_{i,t}\right\} \tag{48a}$$

$$p^1_{i,t} = \max\left\{0, p^2_{i,t}\right\} \tag{48b}$$

$$p^2_{i,t} = \min\left\{IC^E_i \cdot SOC_{\max} - IC^E_i \cdot SOC_{i,t}, IP^{\mathrm{E}}_i\right\} \tag{48c}$$

For the two types of nonlinear terms min(·) and max(·) in Equations (48a)–(48c), the equation is linearized to Equations (49a)–(49c) by introducing an infinite positive value M and auxiliary dummy variables $\mu_1, \mu_2, \mu_3, \mu_4, \mu_5, \mu_6$, respectively.

$$\begin{cases} p^{\mathrm{W}}_{i,t} + p^{\mathrm{PV}}_{i,t} - p^{\mathrm{R2C}}_{i,t} \geq p^{\mathrm{R2E}}_{i,t}, p^1_{i,t} \geq p^{\mathrm{R2E}}_{i,t} \\ p^{\mathrm{W}}_{i,t} + p^{\mathrm{PV}}_{i,t} - p^{\mathrm{R2C}}_{i,t} \leq p^{\mathrm{R2E}}_{i,t} - M(1-u_1), \\ \quad p^1_{i,t} \leq p^{\mathrm{R2E}}_{i,t} - M(1-u_2) \\ u_1 + u_2 \geq 1, u_1, u_2 \in \{0,1\} \end{cases} \tag{49a}$$

$$\begin{cases} p^2_{i,t} \leq p^1_{i,t}, 0 \leq p^1_{i,t} \\ p^2_{i,t} \geq p^1_{i,t} - M(1-u_3), 0 \geq p^1_{i,t} - M(1-u_4) \\ u_3 + u_4 \geq 1, u_3, u_4 \in \{0,1\} \end{cases} \tag{49b}$$

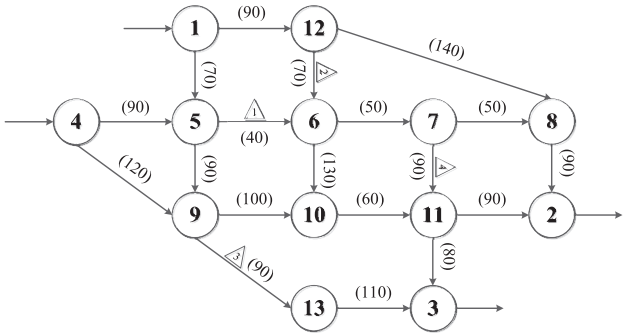

FIGURE 4 The Nguyen-Dupius network with four service areas.

$$\begin{cases} IC^E_i \cdot SOC_{\max} - IC^E_i \cdot SOC_{i,t} \geq p^2_{i,t}, IP^{\mathrm{E}}_i \geq p^2_{i,t} \\ IC^E_i \cdot SOC_{\max} - IC^E_i \cdot SOC_{i,t} \leq p^2_{i,t} - M(1-u_5), \\ \quad IP^{\mathrm{E}}_i \leq p^2_{i,t} - M(1-u_6) \\ u_5 + u_6 \geq 1, u_5, u_6 \in \{0,1\} \end{cases} \tag{49c}$$

Similarly, nonlinear terms of min(·) and max(·) in Equations (25)–(28) are handled with the same procedure. Eventually, the lower model B is transformed into the MILP model.

5.4 | Numerical experiment

This section verifies the convergence and applicability of the proposed H-M-L algorithmic structures.

The Nguyen-Dupius network is shown in Figure 4, where the number in parentheses is the length (unit km) of the road. The velocity and road capacity are set as 100 km/h and 2300 pcu. Four service areas are set on the road (5, 6), (12, 6), (9, 13), (7, 11). The charger capacity thresholds of each service area are set to 8, 10, 8, and 12. The flow rate

ALGORITHM 1 MA-MSA.

Input: Highway network N, charging network R, OD traffic flow $q^t_{o,d}$
Output: the matrices of travel $\mathbf{v}(R)$ and charging demand $\mathbf{f}(R)$

Construct $L^e_{o,d}(N,R)$ according to Equation (1);
for$(t \in T)$ **do**
  Update $TC_x(R)$ and $P_x(R)$. Set $n = 1$;
  for $(o \in O)$ **do**
    for $(d \in D)$ **do**
      Set S_x, $D_{x,t}$ // Label for new EVs
      for $(x \in X_t)$ **do**
        Set $period = 15$;
        if $(f\_time_{x,t} < period)$ **then** // Keep current status
          $D_{x,t+1} = \{L_{x,t}, SOC_{x,t+1}, status_{x,t}, f\_time_{x,t+1} = f\_time_{x,t} - period\}$
        else
          if $(status_{x,t} = C)$ **then** // Leave the station
            $D_{x,t+1} = \{L_{x,t+1} = L_{x,t} + 1, SOC_{x,t+1}, status_{x,t+1} = D, f\_time_{x,t+1} = \tau_{L_{x,t}+1,,t}\}$
          else
            if $(L_{x,t} + 1 = c_x)$ **then** // Enter the station
              $D_{x,t+1} = \{L_{x,t+1} = c_x, SOC_{x,t+1}, status_{x,t+1} = C, f\_time_{x,t+1} = TW_{x,c_l}(R) + TC_{x,c_l}(R)\}$
            elif $(L_{x,t} + 1 = d_x)$ **then** // Leave the highway
              $X_t = X_t - x$
            else // Travel to next road
              $D_{x,t+1} = \{L_{x,t+1} = L_{x,t} + 1, SOC_{x,t+1}, status_{x,t+1} = D, f\_time_{x,t+1} = \tau_{L_{x,t}+1,,t}\}$
            end if
          end if
        end if
      end for
    end for
  end for
  Update $TC_x(R)$ and $P_x(R)$;
  Get the auxiliary flow distribution $\{Y^{t,(n)}_a\}$ // Repeat the simulation (line 3-line 8)
  Update the flow distribution $\{X^{t,(n+1)}_a\}$ // By $X^{t,(n+1)}_a = X^{t,(n)}_a + \lambda^{(n)} \cdot (Y^{t,(n)}_a - X^{t,(n)}_a)$, $\lambda^{(n)} = n/(1+2+3+\cdots+n)$
  Calculate the gap value, and update $n = n + 1$ // By $gap = \sqrt{\sum_{a\in A}(X^{t,(n+1)}_a - X^{t,(n)}_a)^2}/(\sum_{a\in A}(X^{t,(n)}_a))$
  if $(gap < \varepsilon)$ **then**
    break
  end if
end for

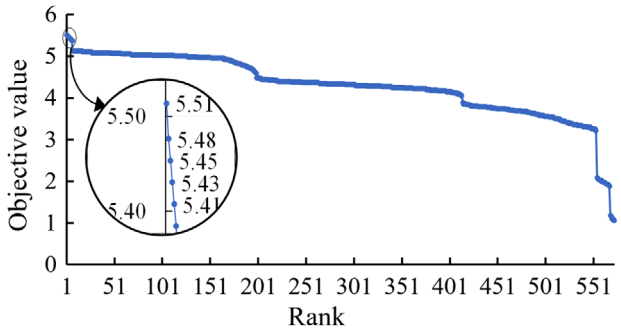

FIGURE 5 The objective values of all feasible solutions.

per 15 min for OD pairs (1, 2), (1,3), (4, 2), and (4, 3) are set to 16, 30, 24, and 16 pcu, respectively. In this case, the wind speed and solar irradiation data are collected from four actual locations.

In this case, the EV percentage is assumed to be 10%. The driving range and battery capacity of the EV are set to 400 km and 60 kWh, respectively. Other parameters of the traffic assignment model are set as follows: $S^0 = 100\%$, $S^1 = 30\%$, $S^2 = 40\%$, $S^{\exp} = 80\%$, $n = 1$, $\alpha^* = 34\text{RMB}/h$, $\beta^* = 1.5\text{RMB/kWh}$, $\theta^* = 1$. The installed capacity thresholds for generation facilities are set to $IC^{W\text{kWh}}_{\max} = 1500$ kWh, $IC^{\text{PV}}_{\max} = 1200$ kWh, and $IC^{E}_{\max} = 1500$ kWh, and the RP supply rate is set to $\mu' = 0.9$. Parameters of the WPS system are set according to Eocyle's Eo10 wind generators and China Sunergy chi285-72 M PV module. $v_{\text{in}} = 2.75$ m/s, $v_{\text{out}} = 20$ m/s, $v_{\text{rate}} = 12$ m/s, $G_{\text{stc}} = 1000$ W/m^2, $T_{\text{stc}} = 25°\text{C}$, $k' = -0.42\%/°C$, $SOC_{\min} = 20\%$, $SOC_{\max} = 90\%$, $P_{\text{ch}} = 120$ kWh. Parameters involved in the upper model are set as follows: $T^{avg} = 5$ min, $T^{\max} = 30$ min, $B_{\min} = 4$, $z^{**}_{\text{cs}} = 2$ million RMB/unit, $z^{**}_{\text{ch}} = 50,000$ RMB/unit, $z^{**}_{\text{tr}} = 357.29$ RMB/kVA, $K^{**}_{\text{ch}} = 0.7$, $L^{**}_{\max} = 0.8$, $\alpha^{**}_{\text{cs}} = 0.85$, $\eta^{**}_{\text{ch}} = 90\%$, $\cos\phi^{**}_{\text{ch}} = 0.95$, $z^{**}_{\text{hr}} = \$12,000$, $z^{**}_{m} = \$59.2/\text{kVA}$, $B_{\max,i} = 10$. The simulation period is 24 h. The time intervals of lower models A and B are 15 min and 1 h, respectively. The parameters with superscript * and ** are set referring to T. Y. Zhang et al. (2022), and Y. Yang et al. (2022), respectively. The case is run on a personal computer configured with Intel Core i7-8650U 1.90 GHz and 16 GB RAM.

The optimal solution is obtained by the enumeration method first. In this case, there are 2876 solutions for the charging network deployment. Due to constraints (43)–(45), 2304 solutions are infeasible. The objective values of the remaining 572 solutions are ranked from best to worst as shown in Figure 5. The objective values vary from 5.51 million to 1.06 million RMB, indicating that the network deployment greatly impacts the operator's revenue.

Then, the GA (Q. Zhang et al., 2023), particle swarm optimization (PSO; Hossain et al., 2019), and simulated

TABLE 2 The final solutions obtained in three algorithms.

Solution	Obj (million RMB)	Rank	G-M-L		S-M-L		P-M-L	
			Time	Iter	Time	Iter	Time	Iter
(1:8, 4:7)	5.51	1	29	19	27	18	28	24
(1:8, 4:8)	5.48	2	1	22	2	23	2	34
(1:8, 4:10)	5.43	4	–	–	1	18	0	–
(1:8, 2:9, 3:7)	4.30	314	–	–	–	–	–	–

annealing (SA) (Siddique & Adeli, 2016) are applied to the H-M-L structure. The G-M-L, S-M-L, and P-M-L algorithms are constructed. The parameters of the three algorithms are set as follows: GA (population = 10, crossover probability = 0.6, and mutation probability = 0.6); SA (initial temperature = 100, final temperature = 3, the attenuation parameter of temperature = 0.95); PSO (population = 15, study factor 1 = study factor 2 = 2, the inertial factor following linear decreasing weight strategy ranges [0.4, 0.8]). The maximum iteration number and the number of iterations with no change of the three algorithms are all set as 50 and 10, respectively.

The experiments are repeated 30 times for each algorithm, and the performances are recorded in Table 2. The "Solution" refers to the charging network's deployment. The solution (1:8, 4:7) means that the No. 1 and No. 4 service areas are built charging stations with 8 and 7 chargers. The "Rank" refers to the rank of the solution in all solutions. The "Time" column means how many times this solution is obtained in 30 experiments. The "Iter" is the average number of iterations to get the solution. The (1:8, 2:9, 3:7) is the scheme with the median objective value among all feasible solutions.

As shown in Table 2, in a total of 90 experiments, the three algorithms find optimal solutions 84 times and sub-optimal solutions within acceptable limits five times. Also, the average number of iterations to get the final solution is 21, much less than the number of full solutions. Several conclusions about the performance of the M-N-L algorithm structure can be made: (i) The M-N-L algorithm can get the optimal or sub-optimal solution with a high computational efficiency. (ii) The structure of the M-N-L algorithm is well applicable to different heuristic algorithms.

6 | AN EMPIRICAL STUDY

6.1 | Description of case scenario

An empirical study is conducted on the highway of Hu-Bao-Wu city agglomeration as shown in Figure 6a. This highway is located in China's Inner Mongolia Autonomous Region, which has vast land and abundant wind and solar resources. The Inner Mongolia 14th Five-Year Plan for Comprehensive Transportation Development and Renewable Energy Development requires the appropriate deployment of HCN-WPE along the highway's service area (Inner Mongolia Autonomous Region Energy Bureau, 2022; Inner Mongolia Autonomous Region People's Government, 2021).

The highway is 1130-km long and has 57 nodes and 72 road sections. There are 11 service areas on the way. The traffic flow data were collected from the highway Electronic Toll Collection system in July 2019 (before coronavirus disease 2019). The collection precision of flow data is 15 min. The single-day traffic volume in this network is 75,285 pcu, and its temporal distribution is depicted in Figure 6b.

The highway is located in the range of 109.89°E to 113.38°E, which experiences varying wind and solar resources across its length. The charger capacity threshold for each service area is shown in Figure 6c and ranges from 9 to 20, indicating significant differences in the natural resource abundance of various service areas on the highway. Therefore, to achieve the goal of SRPRT, the government must plan the HCN-WPE system based on the abundance of natural resources in different regions. The GA parameters are set as pollution = 20, iteration number = 100, the number of iterations with no change = 10, crossover probability = 0.6, and mutation probability = 0.6. The parameter settings for the project are the same as those in Section 5.4, except for the traffic flow data, wind speed and solar irradiation data, charger capacity thresholds, and GA parameters.

6.1.1 | Deployment scheme

The deployment of the final scheme is displayed in Figure 7. The HCN-WPE system consists of five charging stations located in the service areas of No. A, No. B, No. C, No. E, and No. K. Four charging stations are built on the national highway, while one is on the provincial road. The spatial deployment of the charging network should be compatible with the transport network level. With a well-developed charging network, EV users can stick to their original travel plans, even with en-route replenishment events.

Table 3 displays the specific configuration of each station. The analysis shows that: (i) There are a total of

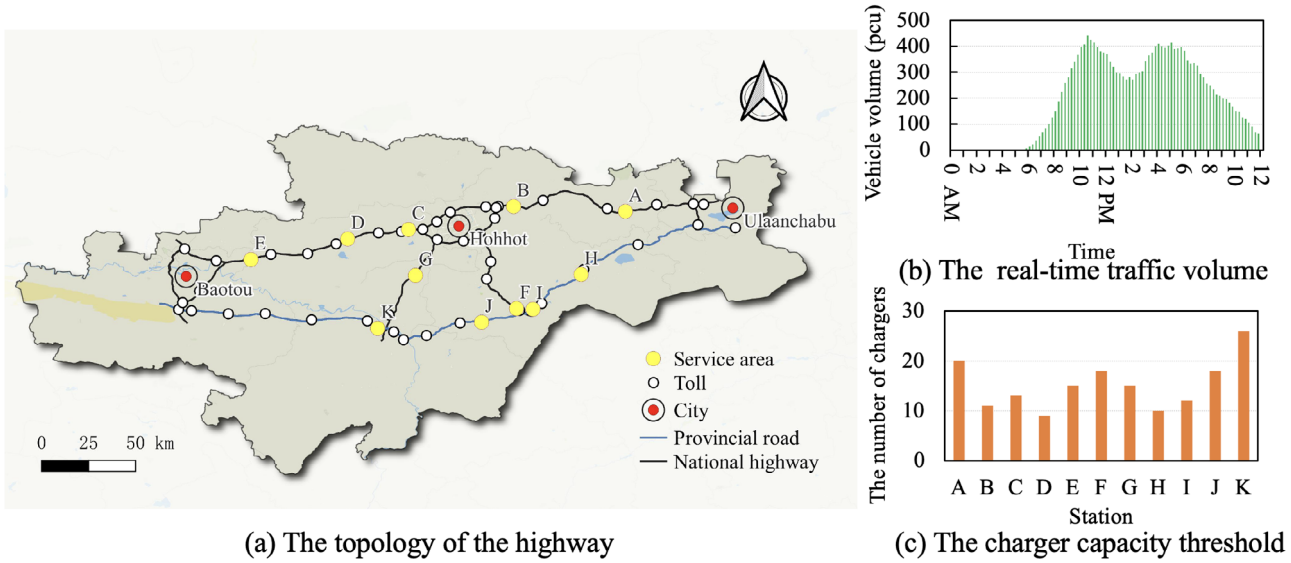

(a) The topology of the highway (b) The real-time traffic volume (c) The charger capacity threshold

FIGURE 6 The basic information of the basic scenario.

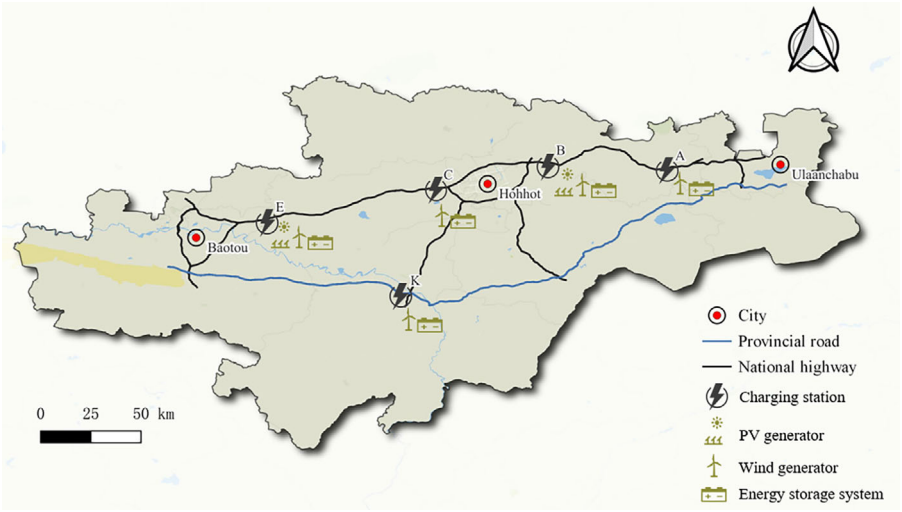

FIGURE 7 The deployment of the HCN-WPE system.

TABLE 3 The configuration of the final planning result.

Charging stations	Configuration				
	$B_i(R)$	$IC_i^{W}(R)$	$IC_i^{PV}(R)$	$IC_i^{E}(R)$	$IP_i^{E}(R)$
A	12	773	0	310	108
B	11	1500	1044	1500	450
C	12	1496	0	1500	450
E	15	579	648	880	264
K	9	442	0	750	225
Network	59	4790	1692	4940	1497

59 chargers installed across five stations. The number of chargers in each station varies from 9 to 15 due to differences in charging load. The load curves of each station are shown in Figure 9a. (ii) Due to its location, Inner Mongolia has more wind resources than solar resources. In the HCN-WPE system, five stations have wind generators with a total installed capacity of 4790 kWh. Only stations B and E have PV generators, with a total installed capacity of 1692 kWh. In contrast, PV generators are built only at stations No. B and No. E, and the total installed capacity is 1692 kWh. (iii) All stations are equipped with ESS, which highlights the importance of ESS in distributed PGSs. Its specific role will be elaborated in Section 3.1.

6.1.2 | Scheme assessment

Then, the operation and planning of the HCN-WPE system are assessed in terms of economy, LOS, and energy benefits.

TABLE 4 The economic evaluation of the final planning result.

Economy (million RMB)	Charging stations					
	A	B	C	E	K	Network
Construction costs	1.35	3.26	2.51	1.80	1.09	10.00
O&M costs	0.26	0.37	0.37	0.31	0.20	1.50
Operation benefits	4.60	4.92	5.51	5.73	4.00	24.74
Salvage benefits	0.04	0.09	0.07	0.04	0.02	0.26
NPV	3.02	1.38	2.70	3.66	2.74	13.50

Abbreviations: NPV, net present value; O&M, operation and maintenance.

TABLE 5 The system level of service (LOS) of the final deployment scheme.

Level of service	Charging stations					
	A	B	C	E	K	Network
No. of vehicles served	357	389	377	447	261	1831
Avg. waiting time (min)	1.28	2.93	3.02	2.68	1.67	2.39
Avg. charging time (min)	18.19	17.67	20.29	18.48	22.12	19.15
Charger utilization	0.42	0.53	0.62	0.46	0.47	0.50

1. Economy

The economic indicators for each station and the overall system are calculated according to Equations (30) and (31) and Equations (37)–(41). The economy of the final deployment scheme is assessed in Table 4. The overall NPV of the HCN-WPE system reaches 13.50 million RMB, indicating a good return on investment. Specific to individual stations, the NPV of each station varies from 1.38 million to 3.66 million RMB due to differences in facility configuration and charging loads across stations. The No. B charging station, with a relatively small profit, is crucial, as it provides the replenishment service for EV travel on the provincial road.

2. Level of service

The proposed lower model A enables real-time simulation and monitoring of the charging facilities' operation. Table 5 and Figure 8 present the static evaluation and dynamic changes of the LOS of each station in the final deployment scheme, respectively.

Throughout the day, 1831 EVs generate charging requests on this highway, accounting for 24.1% of the total EV trips. Since long-distance trips make up only a small proportion of highway trips (Malichová et al., 2022), it is unnecessary to build charging stations in all service areas, particularly in the early stages of EV development. Instead, the charging station should be built to match the limited facility resources with the scattered charging demands by playing the facility's role in demand management and induction.

The left graph in Figure 8 shows the real-time count of vehicles at each charging station. The right graph reveals the station's real-time minimum waiting time and facility utilization. Charging services at each station generally start at 10 a.m. Related to the travel pattern of the traffic flow, the temporal distribution of vehicle count at the stations exists a clear bi-peaks, occurring between 12:00–2:00 and 4:00–8:00 p.m. During the peak periods, the chargers are fully working, and there may be a short queue at the stations.

Overall, the HCN-WPE system provides a high LOS and sustainable charging services. On the one hand, the average waiting time for EV users is around 2.39 min and remains less than 20 min even during peak periods. The HCN-WPE system guarantees the replenishment efficiency for EV users at all times. On the other hand, the facility utilization rate remains below 1.8 during peak periods and averages 0.50 throughout the day. This demonstrates that the charging facilities could operate sustainably throughout the day, avoiding the waste of RP during idle hours and high working pressure during peak hours.

3. Energy benefits

In this section, the energy benefits of the HCN-WPE system are evaluated by analyzing the dynamic operation of each station in the WPE system.

In Figure 9, the right graph displays the hourly power supply composition for chargers at each station. The left graph shows the hourly RP consumption at each station. The red line is the load distribution curve. The analysis reveals that: (i) The charger power mainly originates from wind and PV generators as well as ESS throughout the day, where the RP supply rate of the HCN-WPE system reaches 97.9%. (ii) The RP generation curve matches the EV load distribution quite well. The average RP consumption rate of the HCN-WPE system is approximately 76.6%.

Meanwhile, ESS plays a good role in peak cutting and valley filling as a second-priority power source. Figure 10 presents the charging/discharging status and SOC of ESSs throughout the day. From 12:00 to 8:00 a.m., when the charging load is small, the RP is chiefly stored in storage devices. From 1:00 to 4:00 p.m., when wind/solar resources are abundant, and power generation is much higher than the load, the surplus RP power could be stored in ESSs. The ESS supplies the power to chargers between 11:00 a.m. and 1:00 p.m. and between 4:00 p.m. and 12:00 a.m. when

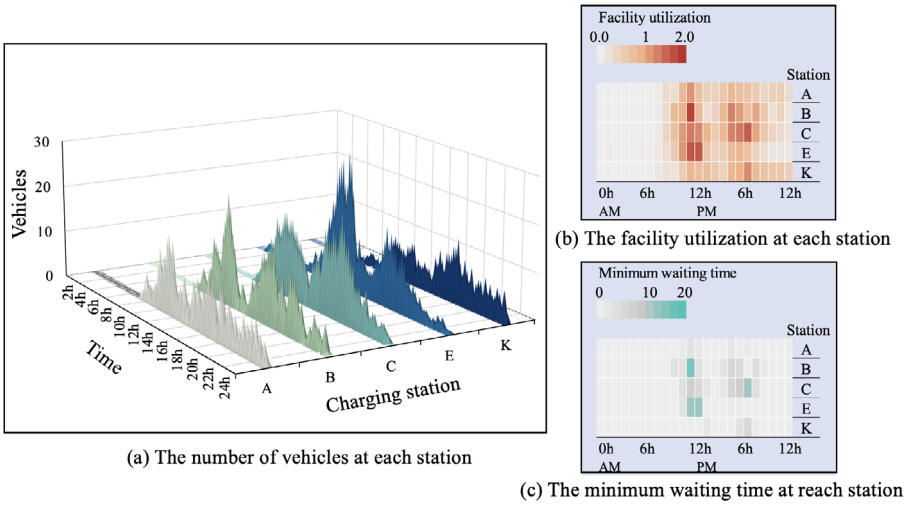

(a) The number of vehicles at each station

(b) The facility utilization at each station

(c) The minimum waiting time at reach station

FIGURE 8 The real-time operation of each charging station.

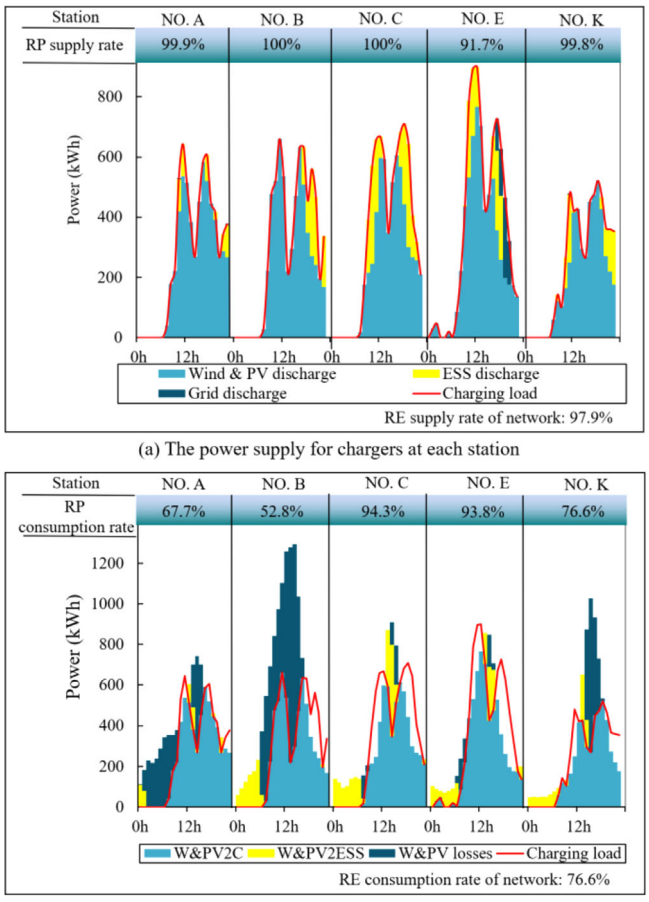

(a) The power supply for chargers at each station

(b) The RE power consumption at each station

FIGURE 9 The dynamic power transmission in the WPE system.

the load is high but natural resources are relatively scarce. And the SOC of the storage equipment is maintained between 30% and 80% throughout the day, guaranteeing the sustainable operation of the ESS.

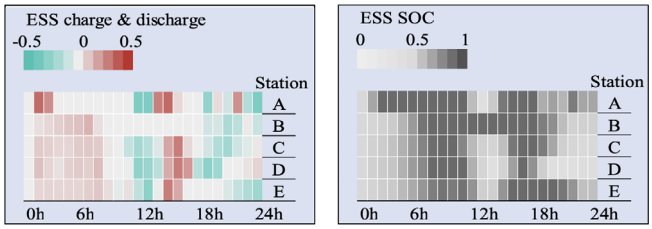

(a) The real-time charge/discharge of ESS

(b) The real-time SOC of ESS

FIGURE 10 The real-time operation of ESS. SOC, status of charge.

In summary, through the coordinated configuration of the WPE system and management of multiple power sources, the PGS could effectively work with the charging station to ensure the efficient use of RE resources while achieving the goal of SRPRT.

6.2 | Effectiveness of the model

In this section, we aim to demonstrate the significance of coordinated planning, network-level planning, and PGS co-configuration through a comparison of different planning models. Six cases with different planning concepts are set up as follows:

Case 1: The proposed nested bi-level planning model for the HCN-WPE system. This model involves joint operation and planning of the HCN-WPE system at the network level.

Case 2: A two-stage planning model for the HCN-WPE system. The first stage optimizes the location and capacity of charging stations to minimize construction costs without considering the abundance of

TABLE 6 The planning results in various cases.

Case	Station locations	$B_i(R)$	$IC_i^{W}(R)$	$IC_i^{PV}(R)$	$IC_i^{E}(R)$	$IP_i^{E}(R)$
1	{A, B, C, E, K}	59	4790	1692	4940	1497
2	{A, B, D, E, K}	55	4758	2794	3390	1026
3	All	Inf	3976	2351	8530	2576
4	{A, B, C, E, K}	59	5230	0	3530	1074
5	{A, B, C, E, K}	59	3801	2228	0	0
6	{A, B, C, E, K}	59	4650	0	0	0

local RE. In the second stage, the configuration of each PWE system is optimized. The two planning stages are done sequentially, where the first stage is optimized by GA and the second stage is solved by Gurobi.

Case 3: A planning model for individual WPE systems. In this case, it is assumed that charging stations with infinite service capacity are built in each service area. Based on the proposed lower model A, the time-sharing load curve of each station is obtained by the MA-MSA algorithm. Then, the configuration of each PWE system is optimized independently by Gurobi.

Cases 4–6: Application of the nested bi-level planning model. The PGS's configurations in Cases 4–6 are wind-ESS, wind-PV, and wind, respectively. They are solved by the proposed G-M-L algorithm.

With the same constraints on system LOS, network accessibility, SRPRT, and so forth, the final schemes of the HCN-WPE system obtained in various cases are listed in Table 6.

6.2.1 | Importance of coordinated planning

The importance of multi-network coordinated planning between power supply facilities and PGS is illustrated by comparing Case 1 and Case 2. Table 7 compares the two schemes in terms of economic and energy benefits.

The economic indicators demonstrate that multi-network coordinated planning could maximize the benefits of multiple entities. Compared with Case 1, the construction costs of charging facilities in Case 2 are more economical. However, in the overall view of the HCN-WPE system, the NPV of the network planned with the step-by-step planning concept is 12.05 million RMB, remarkably smaller than that of the coordinated planning network.

Additionally, the energy benefits from the WPE system are limited because its planning priority is lower than that of the charging network in Case 2. In Case 2, meeting the original SRPRT constraint in the generation system planning for station No. E is challenging. Therefore, with the relaxation of μ', the power supply of this station originates 85% from RE. Overall, the RP supply and consumption rates of the HCN-WPE system in Case 2 are much lower than those in Case 1, with 94.8% and 66.1%, respectively.

TABLE 7 The economy and energy benefits in Cases 1 and 2.

	Case 1	Case 2
Economy (million RMB)		
Construction costs of charging facilities	1.93	1.90
Construction costs of the PGS	8.03	8.32
NPV	13.50	12.05
Energy benefits		
RP supply rate	97.9%	94.8%
RP consumption rate	76.6%	66.1%

Abbreviations: NPV, net present value; RP, renewable power.

6.2.2 | Importance of network-level planning

The role of charging facilities in managing and inducing the charging demands at the network level is illustrated by comparing the final solutions of Cases 1 and 3.

The spatial distribution of charging events within the network is displayed in Figure 11. Results reveal that: (i) Compared with Case 1, Case 3 constructs four additional charging stations but only provides charging services for 139 more EVs. By planning the HCN-WPE system at the network level, the unnecessary charging requests from EV users could be minimized, avoiding the construction of charging stations with low utilization. This improves the economy of the charging network considerably. (ii) In Case 3, the average number of serviced vehicles at each station is 218.9, but the standard deviation is as high as 163.6, causing a large load gap between stations. This leads to a serious imbalance in terms of facilities' operational

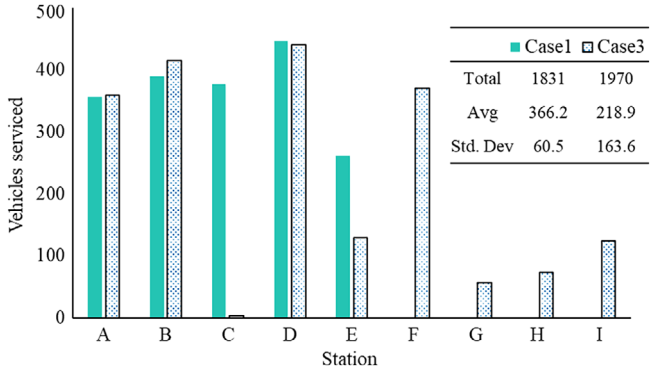

FIGURE 11 The distribution of charging events in Cases 1 and 3.

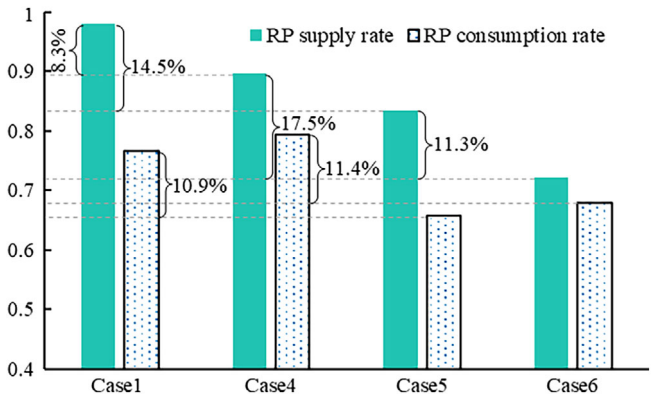

FIGURE 12 The energy benefits in Case 1 and Cases 4–6.

pressure and the investment economy of each station. In Case 1, this imbalance is greatly mitigated by inducing and managing the discrete and differentiated charging demand at the network level.

6.2.3 | Importance of PGS co-configuration

To highlight the importance of PGS co-configuration, we compare the rates of RP supply and consumption between Cases 4–6 and Case 1, shown in Figure 12.

There are two main benefits of the PGS co-configuration. First, co-configuring multiple RP generators can improve the RP supply rate of PGS by utilizing multiple energy sources. The addition of PV generators has resulted in an increase of 11.3% (Case 5) and 8.3% (Case 1) in the supply rate of PGS, compared to Case 6 and Case 4, respectively. Second, due to the temporal volatility of power loads and RE sources, co-configuring RP generators and ESSs can help to utilize the RP more efficiently through the equipment of ESSs to fill power valleys and shave peaks. The results show a 17.5% and 11.4% increase in the supply and consumption rates of PGS in Case 4, compared to Case 6, and a 14.5% and 10.9% increase in Case 1, compared to Case 5, respectively.

7 | CONCLUSION AND DISCUSSION

This study aims to provide an effective planning method for decision-makers in building a high LOS, self-sufficient RP, and sustainable HCN-WPE system. To address the planning problem of the HCN-WPE system with the coupled multi-networks, a nested bi-level optimization model is proposed based on the resolution of the interactions among the networks. It realizes the joint operation and planning of EV users, power supply facilities, and power generation facilities on the highway. An H-M-L algorithm structure, combining the heuristic algorithm, MA simulation technology, and LP algorithm, is designed. The proposed algorithm structure is verified to have good convergence and applicability by comparing the performance of the H-M-L algorithm structure under three different heuristic algorithms on the Nguyen-Dupius network. Additionally, an empirical study in the Hu-Bao-Wu city aggregation is used to illustrate the model's effectiveness and provide decision-makers with insightful guidance for planning and managing the HCN-WPE system. Some important managerial insights are discussed and concluded as follows.

The planner should collaboratively plan the multiple networks involved in the HCN-WPE system at the network level. On the one hand, multi-network coordinated planning effectively improves the investment economy and energy benefits of the whole system. This is the key for the HCN-WPE system to accomplish the SRPRT goal (compared with Case 2, the RP supply and consumption rates within Case 1 increase by 3.2% and 10.5%). On the other hand, network-level planning can effectively manage and induce charging demands through facility deployment. It largely refines the scale of the facility network and helps to balance the load pressure on the stations within the network (compared with Case 3, the standard deviation of station load within Case 1 decreases from 163.6 to 60.5).

When building an independent energy self-sufficient PGS, it is recommended that planners adopt the principles of "adaptation to local conditions" and "co-configuration." The "adaptation to local conditions" principle suggests selecting the appropriate distributed power generation equipment based on the availability of various local RE sources, such as wind, PV, and hydropower. The "co-configuration" principle involves leveraging the complementary power supply of multiple RP generators and the peak cutting and valley filling of ESSs. This will significantly increase PGS's supply and consumption rates.

When planning the HCN-WPE system, it is necessary to consider not only the economy of investment but also the construction equity to guarantee the accessibility of EV travel. However, this may result in notable variations in annual returns for different stations. For example, the station NPV could range from 1.38 million to 3.66 million RMB in Case 1. To ensure the HCN-WPE system is sustainably planned and operated, it is essential to establish a fair and reasonable revenue-sharing system for the stations.

There are still some things that could be improved. First, the uncertainties of the traffic situation and RE resources should be considered in the HCN-WPE planning. Second, exploring the impact of critical factors, such as facility costs, charging technology, and EV penetration, on the investment and management of HCN-WPE systems is one of the future research directions. Third, parameters such as land use and socioeconomics could be incorporated into the refined modeling of EV users' travel behavior.

ACKNOWLEDGMENTS

This work was supported by the National Natural Science Foundation of China 52172312, the Fundamental Research Funds for the Central Universities 2023YJS151, the National Natural Science Foundation of China 71931003, Singapore Ministry of Education Academic Research Fund (AcRF) Tier 1 project RT22/22.

REFERENCES

Ali, A., Mahmoud, K., & Lehtonen, M. (2022). Optimal planning of inverter-based renewable energy sources towards autonomous microgrids accommodating electric vehicle charging stations. *IET Generation, Transmission & Distribution*, *16*(2), 219–232.

Azin, B., Yang, X. T., Marković, N., & Liu, M. (2021). Infrastructure enabled and electrified automation: Charging facility planning for cleaner smart mobility. *Transportation Research Part D: Transport and Environment*, *101*, 103079.

China Energy. (2022). *Transport and energy integration development report 2022*. http://m.news.cn/hb/2022-12/03/c_1129181070.htm

Domínguez-Navarro, J. A., Dufo-López, R., Yusta-Loyo, J. M., Artal-Sevil, J. S., & Bernal-Agustín, J. L. (2019). Design of an electric vehicle fast-charging station with integration of renewable energy and storage systems. *International Journal of Electrical Power & Energy Systems*, *105*, 46–58.

Fathabadi, H. (2020). Novel stand-alone, completely autonomous and renewable energy based charging station for charging plug-in hybrid electric vehicles (PHEVs). *Applied Energy*, *260*, 114194.

Ferro, G., Minciardi, R., Parodi, L., & Robba, M. (2021). Optimal planning of charging stations in coupled transportation and power networks based on user equilibrium conditions. *IEEE Transactions on Automation Science and Engineering*, *19*(1), 48–59.

Gan, W., Shahidehpour, M., Guo, J., Yao, W., Paaso, A., Zhang, L., & Wen, J. (2020). Two-stage planning of network-constrained hybrid energy supply stations for electric and natural gas vehicles. *IEEE Transactions on Smart Grid*, *12*(3), 2013–2026.

Gan, W., Shahidehpour, M., Yan, M., Guo, J., Yao, W., Paaso, A., Zhang, L., & Wen, J. (2020). Coordinated planning of transportation and electric power networks with the proliferation of electric vehicles. *IEEE Transactions on Smart Grid*, *11*(5), 4005–4016.

Gan, W., Yan, M., Yao, W., Guo, J., Fang, J., Ai, X., & Wen, J. (2021). Multi-network coordinated hydrogen supply infrastructure planning for the integration of hydrogen vehicles and renewable energy. *IEEE Transactions on Industry Applications*, *58*(2), 2875–2886.

Hajibabai, L., Atik, A., & Mirheli, A. (2023). Joint power distribution and charging network design for electrified mobility with user equilibrium decisions. *Computer-Aided Civil and Infrastructure Engineering*, *38*(3), 307–324.

He, J., Yang, H., Tang, T. Q., & Huang, H. J. (2018). An optimal charging station location model with the consideration of electric vehicle's driving range. *Transportation Research Part C: Emerging Technologies*, *86*, 641–654.

Henrique, L. F., Silva, W. N., Silva, C. C., Dias, B. H., Oliveira, L. W., & de Almeida, M. C. (2023). Optimal siting and sizing of distributed energy resources in a Smart Campus. *Electric Power Systems Research*, *217*, 109095.

Hossain, S. I., Akhand, M. A. H., Shuvo, M. I. R., Siddique, N., & Adeli, H. (2019). Optimization of university course scheduling problem using particle swarm optimization with selective search. *Expert systems with applications*, *127*, 9–24.

IEA. (2023). *Tracking clean energy progress 2023*. IEA. https://www.iea.org/reports/tracking-clean-energy-progress-2023

Inner Mongolia Autonomous Region Energy Bureau. (2022). *Inner Mongolia Autonomous Region "Fourteenth Five-Year Plan" about Renewable Energy Development Plan*. http://www.als.gov.cn/art/2022/8/2/art_73_445548.html

Inner Mongolia Autonomous Region People's Government. (2021). *Inner Mongolia Autonomous Region "Fourteenth Five-Year Plan" about Comprehensive Transportation Development Plan*. https://www.nmg.gov.cn/zwgk/zfxxgk/zfxxgkml/202110/t20211019_1911901.html

Kchaou-Boujelben, M. (2021). Charging station location problem: A comprehensive review on models and solution approaches. *Transportation Research Part C: Emerging Technologies*, *132*, 103376.

Li, C., Zhang, L., Ou, Z., Wang, Q., Zhou, D., & Ma, J. (2022). Robust model of electric vehicle charging station location considering renewable energy and storage equipment. *Energy*, *238*, 121713.

Liu, C., Chau, K. T., Wu, D., & Gao, S. (2013). Opportunities and challenges of vehicle-to-home, vehicle-to-vehicle, and vehicle-to-grid technologies. *Proceedings of the IEEE*, *101*(11), 2409–2427.

Malichová, E., Cornet, Y., & Hudák, M. (2022). Travellers' use and perception of travel time in long-distance trips in Europe. *Travel Behaviour and Society*, *27*, 95–106.

Mowry, A. M., & Mallapragada, D. S. (2021). Grid impacts of highway electric vehicle charging and role for mitigation via energy storage. *Energy Policy*, *157*, 112508.

National Development and Reform Commission. (2022). *Plan for modern energy system during the 14th five-year period*. https://www.ndrc.gov.cn/xxgk/zcfb/ghwb/202203/t20220322_1320016.html

Nguyen, V. C., Wang, C. T., & Hsieh, Y. J. (2021). Electrification of highway transportation with solar and wind energy. *Sustainability*, *13*(10), 5456.

Nishanthy, J., Charles Raja, S., Praveen, T., Jeslin Drusila Nesamalar, J., & Venkatesh, P. (2022). Techno-economic analysis of a hybrid

solar wind electric vehicle charging station in highway roads. *International Journal of Energy Research*, *46*(6), 7883–7903.

Siddique, N., & Adeli, H. (2016). Simulated annealing, its variants and engineering applications. *International Journal on Artificial Intelligence Tools*, *25*(6), 1630001.

Smith, M. J. (1979). The existence, uniqueness and stability of traffic equilibria. *Transportation Research Part B: Methodological*, *13*(4), 295–304.

Sun, B. (2021). A multi-objective optimization model for fast electric vehicle charging stations with wind, PV power and energy storage. *Journal of Cleaner Production*, *288*, 125564.

Sun, Q., Wu, Z., Gu, W., Liu, P., Wang, J., Lu, Y., Zheng, S., & Zhao, J. (2022). Multi-stage co-planning model for power distribution system and hydrogen energy system under uncertainties. *Journal of Modern Power Systems and Clean Energy*, *11*(1), 80–93.

The CPC Central Committee and the State Council. (2019). *The program of building national strength in transportation*. http://www.gov.cn/zhengce/2019-09/19/content_5431432.htm

Unterluggauer, T., Rich, J., Andersen, P. B., & Hashemi, S. (2022). Electric vehicle charging infrastructure planning for integrated transportation and power distribution networks: A review. *ETransportation*, *12*, 100163.

Wang, X., Shahidehpour, M., Jiang, C., & Li, Z. (2018). Coordinated planning strategy for electric vehicle charging stations and coupled traffic-electric networks. *IEEE Transactions on Power Systems*, *34*(1), 268–279.

Xia, F., Chen, H., Li, H., & Chen, L. (2022). Optimal planning of photovoltaic-storage fast charging station considering electric vehicle charging demand response. *Energy Reports*, *8*, 399–412.

Yang, W., Liu, W., Chung, C. Y., & Wen, F. (2020). Joint planning of EV fast charging stations and power distribution systems with balanced traffic flow assignment. *IEEE Transactions on Industrial Informatics*, *17*(3), 1795–1809.

Yang, Y., Zhang, T., Zhu, Y. T., & Yao, E. J. (2022). Optimal deploying of charging systems on an expressway network considering the optimal construction time sequence and the charging demand. *Journal of Tsinghua University (Science & Technology)*, *62*(7), 1163–1177.+1219. (In Chinese).

Zeng, B., Dong, H., Sioshansi, R., Xu, F., & Zeng, M. (2020). Bilevel robust optimization of electric vehicle charging stations with distributed energy resources. *IEEE Transactions on Industry Applications*, *56*(5), 5836–5847.

Zeng, T., Zhang, H., & Moura, S. (2019). Solving overstay and stochasticity in PEV charging station planning with real data. *IEEE Transactions on Industrial Informatics*, *16*(5), 3504–3514.

Zhang, Q., Yu, H., Zhang, G., & Ma, T. (2023). Optimal planning of flood-resilient electric vehicle charging stations. *Computer-Aided Civil and Infrastructure Engineering*, *38*(4), 489–507.

Zhang, T. Y., Yang, Y., Zhu, Y. T., Yao, E. J., & Wu, K. Q. (2022). Deploying public charging stations for battery electric vehicles on the expressway network based on dynamic charging demand. *IEEE Transactions on Transportation Electrification*, *8*(2), 2531–2548.

Zhang, T. Y., Yao, E. J., Yang, Y., Pan, L., Li, C. P., Li, B., & Zhao, F. (2023). Deployment optimization of battery swapping stations accounting for taxis' dynamic energy demand. *Transportation Research Part D: Transport and Environment*, *116*, 103617.

Zhang, X., Rey, D., & Waller, S. T. (2018). Multitype recharge facility location for electric vehicles. *Computer-Aided Civil and Infrastructure Engineering*, *33*(11), 943–965.

Zhao, D., Li, X., & Cui, J. (2021). A simulation-based optimization model for infrastructure planning for electric autonomous vehicle sharing. *Computer-Aided Civil and Infrastructure Engineering*, *36*(7), 858–876.

How to cite this article: Zhang, T.-Y., Yao, E.-J., Yang, Y., Yang, H.-M., & Wang, D. Z. W. (2024). Multi-network coordinated charging infrastructure planning for the self-sufficient renewable power highway. *Computer-Aided Civil and Infrastructure Engineering*, 1–24. https://doi.org/10.1111/mice.13196

APPENDIX

Abbreviation	
RE	Renewable energy
RP	Renewable power
SRPRT	Self-sufficient renewable energy road transport
PV	Photovoltaic
ESS	Energy storage system
WPE	Wind-PV-ESS
HCN-WPE	Highway charging network with the Wind-PV-ESS
LOS	Level of service
EV	Electric vehicle
NPV	Net present value
MA	Multi-agent-based
LP	Linear programming
H-M-L	A heuristic algorithm, MA simulation, and LP algorithm
OD	Origin and destination
PGS	Power generation system
MINLP	Mixed integer nonlinear programming
MILP	Mixed integer linear programming
DTA	Dynamic traffic assignment
SDUE	Stochastic dynamic user equilibrium
MA-DTA	Multi-agent-based dynamic traffic assignment
MA-MSA	Multi-agent-based method of successive averages
SOC	Status of charge
O&M	Operation and maintenance
GA	Genetic algorithm
PSO	Particle swarm optimization
SA	Simulated annealing

Sets	
N, R:	the highway and charging network
C, D:	the set of origin and destination
A, ϕ:	the set of road sections and service areas
$\phi(R)$:	the location of stations on network R
T, T':	the sets of simulation periods in the lower model A and B
X:	the set of EVs, $x \in X$
X_t:	the set of EVs in the network at time t
$L^g_{o,d}(N)$:	the set of effective routes for gasoline vehicles between (o, d)
$L^e_{o,d}(N, R)$:	the set of effective routes for EV between (o, d)
$EE(o), ES(o)$:	the set of roads ending and starting at node o
{W, PV, E}:	the set of devices, $m \in$ {W, PV, E}
Parameters	
S^1, S^2:	the minimum SOC thresholds while EV driving and leaving the highway
$S^0, S^{\exp}$:	the initial SOC and the expected SOC after leaving stations
n:	the maximum number of charging times
α, β:	the time value of EV users and charging price
θ:	the discrete coefficient reflecting user perception differences
$\Delta l_a, \Delta l_l$:	the lengths of road a and route l
C_a, t_a:	the traffic capacity and free-flow travel time of road a
$\partial_{a,l}$:	the binary variable to judge whether road a is part of route l. If it is then $\partial_{a,l} = 1$; otherwise, $\partial_{a,l} = 0$
Δt:	the time step
$\upsilon_{\text{in}}, \upsilon_{\text{out}}, \upsilon_{\text{rate}}$:	the cut-in wind speed, cut-out wind speed, and rated wind speed
$G_{\text{stc}}, T_{\text{stc}}$:	the solar irradiation and temperature under the standard conditions
k':	the temperature coefficient
η:	the power efficiency
R^{S}, R^G:	the benefits per unit of sold electricity from RP generators and the grid
$U^A_{\text{W}}, U^A_{\text{PV}}$:	the costs per unit of installed capacity for wind and PV generators
U^A_E, U^Q_E:	the costs per unit of rated power and of installed capacity of the ESS
U^C_m, D_m:	the investment cost of the converter and the salvage value of device m
$M^{\text{A}}_m, M^{\text{C}}_m$:	the annual O&M costs of the units and converters of device m
R^{EN}:	the environmental benefit per unit of RP
L_m:	the lifespan of each device
Parameters	
$SOC_{\min}, SOC_{\max}$:	the lower and upper thresholds of ESS's SOC in operation
r:	the funding discount rate
μ':	the RP supply rate
δ':	the initial SOC of ESSs during the day
$IC^m_{\max}$:	the maximum installed capacities of device m
$z_{\text{cs}}, z_{\text{ch}}, z_{\text{tr}}$:	the construction costs of station and charger and the capacity cost of distribution equipment
RP_{ch}:	the rated power of fast chargers
K_{ch}:	the simultaneous rate of charging
$L_{\max}$:	the daily maximum load rate of the individual station
α_{cs}:	the ratio of charging load to total load at the station
η_{ch}:	the charging efficiency
z_m:	the average annual O&M cost per unit of distribution equipment capacity
$T^{\text{avg}}, T^{\max}$:	the preset average waiting time and maximum waiting time
$\cos\phi_{\text{ch}}$:	the power factor of chargers
z_{hr}:	the average annual labor cost per charger
Variables	
$PC_{x,l}(R)$:	the probability that EV x chooses route l on network R
$TC_{x,l}(R)$:	the generalized travel cost of route l for EV x on network R
$M_{o,d,l}$:	the correction term of route l
L_x:	the route for EV x
$\tau_{a,t}$:	the travel time of road a at time t
$H_{x,c_i}(R)$, $TW_{x,c_i}(R)$, $TC_{x,c_i}(R)$:	the charging volume, queuing time, and charging time of EV x at station i
$t^{\text{pile}}_{c_i,b,t}(R)$:	the working finishing time of charger b at station i at time t
$t^{\text{l}}_{x,c_i}(R), TW_{x,c_i}(R)$, $TC_{x,c_i}(R)$:	the departure moment, queuing time, and charging time
$S_{x,c_i}(R)$:	the SOC of EV x arriving at station i
$t^{\text{a}}_{x,c_i}(R), t^{\text{l}}_{x,c_i}(R)$:	the moments when EV x arrives and leaves station i
$\mu^t_{o,d}(R)$:	the minimum expected travel cost on (o, d) at time t
$q^t_{o,d}$:	the new loading flow on (o, d) at time t

$u^t_{o,d,l}$, $v^t_{o,d,l}$:	the outflow rate and inflow rate of choosing route l on (o, d) at time t
X^t_a:	the number of vehicles on road a at time t
u^t_a, v^t_a:	the outflow rate and inflow rate of road a at time t
d^t_a:	the number of EVs at the station built on road a at time t
$f^t_{o,d,l}$:	the new loading flow choosing route l on (o, d) at time t
$f^{t,*}_{o,d,l}$:	the optimal solution of $f^t_{o,d,l}$
$p^m_{i,t}$:	the power of device m at station i in time t
IC^m_i:	the installed capacities of device m at station i
$v'_{i,t}$:	the wind speed at station i in time t
$G_{i,t}$, $T_{i,t}$:	the real-time solar irradiation and temperature at station i in time t
IP^{E}_i:	the rated output power of ESSs at station i
$SOC_{i,t}$:	the real-time SOC of ESSs at station i in time t
$p^{\mathrm{R2C}}_{i,t}$, $p^{\mathrm{R2E}}_{i,t}$:	the input powers from the RP generators to chargers and to the ESS at station i in time t
$p^{\mathrm{D}}_{i,t}$:	the load demand at station i in time t
$p^{\mathrm{E2C}}_{i,t}$, $p^{\mathrm{G2C}}_{i,t}$:	the input powers from the ESS and the grid to chargers at station i in time t
$C_{i,m}$:	the annual investment and O&M cost of device m
$NPV^{\mathrm{WPE}}_i(R)$:	the NPV of WPE system at location i on network R
$NPV^{\mathrm{HCN-WPE}}(R)$:	the NPV of HCN-WPE system on network R
$IC^{\mathrm{W}}_i(R), IC^{\mathrm{PV}}_i(R), IC^{\mathrm{E}}_i(R), IP^{\mathrm{E}}_i(R)$:	the optimal WPE configurations on network R
$B_i(R)$:	the number of chargers at station i on network R
$S^{\mathrm{ET}}_i(R)$:	the capacity of power distribution equipment at station i on network R
$B_{\max,i}$:	the maximum threshold for the number of chargers at station i
$\mathbf{v}(R)$, $\mathbf{f}(R)$:	the matrices of travel and charging demand decisions when the system reaches the SDUE status on network R
$y_i(R)$:	the binary variable to determine whether a charging station is built at station i on network R. If it is built then $y_i(R) = 1$; otherwise, $y_i(\mathbb{R}) = 0$.